THE OPTICAL PROPERTIES OF RARE EARTH METALS

B. Cleyet

A thesis submitted to the University of Keele
in partial fulfilment of the requirements for
the degree of Doctor of Philosophy.

1973

This Thesis describes experimental work done by the author under the direction of Dr. J. N. Hodgson at the University of Keele, Physics Department.

ACKNOWLEDGEMENTS

I would like express my thanks to the following:

Professor D.J.E. Ingram, for providing facilities for research in his department.

Dr. J.N. Hodgson, for his assistance and supervision of the work.

Other members of the Physics Department, University of Keele, particularly Mr. F. Rowerth and Mrs. K. Merifield.

The University of Keele, for providing financial support in the form of a University Demonstratorship.

I would also like to thank Dr. S.H. Liu and Dr. J.P. Petrakien.

Finally my thanks are also due to Dr. H. Richards, Dr. J. Eades, Mr. M. Cooper, Dr. L. Catalán, Professor Skinner and Norma Mufuco.

ABSTRACT

Ellipsometric measurements at the film-substrate interface of the optical constants of five lanthanide metals, (Nd, Gd, Tb, Dy and Yb), have been made within 0.5 and 5.5eV. General agreement was found with theoretically predicted conductivity from A.P.W. energy band calculations and the experimental data. The change in σ due to the magnetic ordering of Gd, Tb and Dy was assumed to be due to the creation and destruction of available transitions caused by a rigid splitting of the bands. Surprisingly good agreement was found with this model.

PREFACE

This thesis describes the results and interpretation of optical measurements on evaporated films of five lanthanide metals. Previously published work in this field is limited to measurements of 8 rare earth metals (Nd, Sm, Eu, Gd, Dy, Ho, Yb, and Lu). The present work gives values for the optical constants of neodymium, gadolinium, terbium, dysprosium, and ytterbium within the silica transmission band, ($\hbar w = 0.5 \rightarrow 5.5$ eV). These measurements represent an advance over previous work either because of the greater spectral range, or measurement at low (ℓN_2) temperature in addition to room temperature, or because of greater accuracy of results due to a superior method of measurement and higher purity metal.

Unless measurements are made in ultrahigh vacuum, ($< 10^{-9}$ torr) on rather thin films ($0.02\text{-}0.1\ 10^{-6}$ m), metal films must be measured by a reflection method. The reflection polarimetry method due to Drude gives the optical constants directly and was used for this work. By only one of the previously published authors was this method used though it is significantly more accurate and convenient than the other methods reported. This is especially true when an internal reflection method is used to measure films deposited on glass prisms in a manner introduced by Ives and Briggs, (1936).

The theory necessary for deduction of optical constants from reflection polarimetry is given in the first chapter. The second describes the theory, classical and quantum mechanical, necessary to infer the electronic structure of metals from their optical constants. The third describes the apparatus and experimental method. The fourth

chapter deals with previous and present measurements including a comparative discussion of the results. The fifth deals with an interpretation of the optical data in an attempt to describe the electronic (band) structure of the rare earth metals.

INTRODUCTION

The rare earths form an unusual group of elements. Until recently they found little use because they were not easily separable from each other and from uranium and thorium with which they are most commonly associated. It is for this reason that they are called "rare" as the least abundant is more common than gold. Because many of the rare earths have high neutron absorption cross sections and are a significant fission product, it was necessary that commercial methods of separation be developed. As a result sixteen new metals, including the electronic and chemically similar yttrium and scandium, have become commercially available. The sudden availability of the rare earth metals with their distinctive properties has resulted in a research explosion. Already much is known about their electrical, chemical, magnetic, and spectroscopic properties.

Their distinctive and anomalous properties result from their position in the periodic table as forming the third of five transition series. Unlike the first two series the succeeding members after lanthanum are formed, with two exceptions, by adding electrons to the 4-f shell instead of the 5-d. Hence, the rare earths are an inner transition series. The actinides are also an inner transition series the relevant shell being the 5-f shell. Table 1, summarizes the above by giving the electronic configuration of the first member of each series. Note that the lanthanides act as the first member of the third outer transition series whose second member is hafnium.

The lanthanides form an inner transition series because of the imperfect shielding of one 4-f electron by another 4-f electron. This

Table 1 - Transition Series' First Members

Element	atomic number	configuration of outer elecs.
scandium	21 (1st outer)	$3d^1$ $4s^2$
yttrium	39 (2nd outer)	$4d^1$ $5s^2$
lanthanum	57 (1st inner)	$5d_2^1$ $6s_2^2$
hafnium	72 (3rd outer)	$5d$ $6s$
actinium	89 (2nd inner)	$6d^1$ $7s^2$

is due to the shape of the f orbital. As a result the effective nuclear charge experienced by the 4-f electrons steadily increases and the 4-f binding energy becomes too great to allow continuation of the filling of the 5-d shell. Instead a progressively deeper well near the nucleus appears after lanthanum, so that the energy and spatial extension of the 4-f eigenfunction drop sharply. Mayer (Wyborne, 1965) has calculated the binding energy of the 4-f eigenfunction to be -0.95 eV for La (z=57), while for neodymium (z=60) it has dropped to -5 eV. This does not occur for s, p, or d electrons. Consequently the 4-f shell which is being filled does not participate in chemical bonding, in contrast to the first two series', but may interact through the "conduction" electrons to produce long range magnetic order. Direct evidence of the lanthanide "contraction" is shown in electron spin resonance and positron annihilation experiments. However, the "actinide" contraction is less pronounced. For in the electron spin resonance of UF_3 dispersed in CaF_2 hyperfine structure is observed due to the interaction of the 5-f electrons of U^{+3} with fluorine nuclei. While in the corresponding experiment with NdF_3

in CaF_2 it is absent. Further evidence of the 4-f well is that the majority of positron annihilations are with the conduction electrons. In fact the mean life of positrons is $2.95 \pm 0.03 \times 10^{-10}$ sec for lanthanum and $2.90 \pm 0.04 \times 10^{-10}$ sec for lutetium with zero and fourteen 4-f electrons respectively (Rodda and Stewart, 1963). A summary of some physical data for the rare earths is given in Table 2.

In contrast to the detailed electronic knowledge of the transition metals only a superivicial knowledge is available for the REM's. This is because of the difficulty of obtaining sufficiently high purity single crystals for the standard methods of determining the Fermi surface. However, a priori calculations of transition metal band structures have been recently successfully compared to experimental measurements. This has encouraged similar calculations for the REM's; a number of which are now available (Dimmock, 1971). Also the work of Ehrenreich and Philipp (1962) has shown that it is possible to analyze optical data and obtain a superficial knowledge of electronic structure. Optical measurements give less specific information because the constants are related to the sum of all allowed transitions at a specific photon energy. However, they are relatively insensitive to purity. Most importantly, in respect to the REM's useful information may be found at temperatures where the metals are paramagnetic, as well as ordered, whereas the usual methods require very low temperatures where nearly all the REM's are magnetically ordered. Therefore, it may be possible to add to the understanding of the relationship of the conduction electrons and the magnetic structures. Because of the foregoing and a theoretical prediction of Miwa, ((to be elaborated upon later), on optical absorption due to

Table 2 - Physical Data

Element	T_C (^oK)	T_N (^oK)	g_J (Bohr magneton)	eff. (Bohr magneton)	%diff.	mp. (^oC)	bp. (^oC)	structure
La						920	3469	HCP (ABACA..)
Ce		125	15/7	.62	-71	795	3468	as La/FCC below 80oK
Pr	8.7 (FCC)	25	16/5	1.	-69	935	3127	as La
Nd	29 (FCC)	19.	36/11	2.3	-30	1024	3027	as La
Sm		15	5/7			1072	1900	HCP (ABCB CACAB..)
Eu		91	7	7.9	+12	826	1439	BCC
Gd	293		7	7.55	8	1312	3k	HCP (ABAB..)
Tb	219	229	9	9.34	4	1356	2800	as Gd
Dy	85	178	10	10.2	2	1407		as Gd
Ho	20	132	10	10.34	3	1461	2600	as Gd
Er	196	85	9	9.9	10	1497	2900	as Gd
Tm	25	58	7	7.56	8	1545	1727	as Gd
Yb						825	1427	FCC/HCP below 270^oK
Lu						1652	3327	as Gd

antiferromagnetic order, C. Schüler performed an optical study of several REM's. This optical work in general agreed with band structure calculations previously done in a successful attempt to explain the REM's unusually high saturation magnetism and electronic specific heat, (Dimmock, 1964); positron annihilation, (Gustafson, 1964 ; Williams 1968) Was also used to elucidate electronic structure. Again this experimental work was compared to theoretical calculations of band structure and general agreement was found. This combined with resistivity, specific heat, magneto-resistance, and neutron diffraction studies result in a generally agreed upon view of the electronic structure of the rare earth metals. As a result optical data principally serves to verify and possibly add detail to the model. A brief examination of the contribution to what is known by the foregoing follows. Among the first experimental data obtained on the REM's was that of resistivity as a function of temperature. Such plots immediately reveal phase and magnetic transformations. Specific heat plots can then indicate the type of anomaly. In general a Néel point is marked by a lambda type anomaly while a curie point by a symmetrical peak.

The data in Table 2 suggests that the metals may be conveniently divided into two groups - the light and heavy metals. The division is between europium and gadolinium. The heavy metals have rather similar physical properties, with the exception of ytterbium. This is because Yb would normally lack one electron for a filled 4-f shell, but the remaining 4-f orbital is of lower energy than the 5-d and Yb is, therefore, divalent and has fcc structure. In most of its physical and chemical properties it is not a lanthanide but a homologue of strontium. The other heavy

lanthanons become ferromagnetic; the Curie temperature decreases with increase in the atomic number. Ytterbium and lutecium are of course only weakly paramagnetic having filled 4-f shells. (High purity Yb at low temperature undergoes a phase change in which it becomes strongly diamagnetic.) (Bucher, [1970].2 3911] 1970). With the exception of Gd they also exhibit antiferromagnetic order before they become ferromagnetic; again the Néel temperature decreases with increasing atomic number. The light metals have not been investigated to the extent of the heavy possibly because they exhibit irregular properties and are, therefore, not as amenable to theoretical analysis. (Also they are considerably more reactive and, therefore, more difficult to prepare for experiment.) This irregularity may be due to the fact that the 4-f orbitals have a greater extension and variably influence the conduction band. This lack of "localization" may be shown by the fact that only two of the light metals, praseodymium and neodymium (fcc) are ferromagnets, and then only with great difficulty. (Bucher, [1969]:? 1260] 1969). This may also explain why atomic magnetic moments are only slightly lower than the saturation magnetic moments in the HREM while the LRE atomic moments are so much larger than the corresponding metals. Again one of the members of the series is divalent as a half filled f-shell is unusually stable. As a result europium instead of having 6 4-f electrons has 7, the seventh coming from the d shell. Like Ba, Eu is body cc. Eu's rather higher Néel temperature may be due to its more localized 4-f electrons. However, no ferromagnetic state has been reported. Lanthanum of course does not exhibit magnetic order and is a superconductor. ($4.7^{\circ}K$) The others of the series have low Néel temperatures. But for the two divalent exceptions already noted all the rem's have at some

temperature

temperature a hcp structure. Scandium and yttrium atoms have outer shells consisting of a complete s-shell and a d-shell with a single electron. As metals they also have hcp structure. This suggests that the hcp form is a characteristic of a three electron s-d conduction band. Furthermore, Sc and Y have a normal hexagonal structure (ABAB...) as do the heavy REM's. On the other hand the influence of the less than half filled 4-f shell of the light metals results in complicated hcp structures and at lower temperature or high pressure a cubic structure. Samarium has a rhombohedral allotrope. Spectroscopy indicates that the lanthanide atoms regularly add electrons to the 4-f shell with increasing atomic number. Except for exceptions already mentioned this is true for the metals. In fact the magnetic moment per atom deduced from the temperature dependence of the paramagnetic susceptibility is in good agreement with that of the trivalent ions. Therefore, as metals the outer three s,d-electrons become itinerant, while the 4-f electrons are surrounded by 5-s and 5-p filled shells. As a result LS coupling is more important than the crystalline field. Even in the metals the "good" quantum number is the total angular momentum $J = L + S$. That the conduction band is of s-d character is obvious because Hall coefficient values assuming a single band model give very inconsistent results. (Anderson, 1958). The values for the effective number of carriers per atom given by the reference are: Lu-3.5; Yb-0.69; Tm-1.1 negative carriers while samarium has positive carriers below 150°K and negative above. Obviously a two band model is necessary to explain electric and magneto-electric behavior. For two band conduction the ordinary Hall coefficient R_0 is given by:

$$R_0 = \frac{1}{NQ_e} \frac{N_s - N_d(U_d/U_s)^2}{(N_s + N_d\, U_d/U_s)^2}$$

where N is the number of atoms per unit volume, Q_e the unit charge, N_d and N_s the number of carriers contributed by the s and p-d bands per atom respectively, and U_s and U_d their respective mobilities. In this case it is assumed that the s band is nearly full and it contributes holes while the d band is nearly empty and accordingly contributes electrons. Assuming three electrons available for conduction the relation for N_d and N_s is: $N_d = 1 + N_s$. In an earlier paper (Kevane, 1953) the authors) the [illegible] give a plot of N_s as a function of the mobility ratio U_d/U_s, using the previous equation and their experimental values of R_0.

The various curves for Ce are due to the thermal hysteresis of the hcp-fcc transition The low temperature form (fcc) is thought to be due to the promotion of the 4-f electron to the conduction band. Therefore, the appropriate equation is: $N_d = 2 + N_s$. Note the contrast in behavior of the light and heavy metals. Also as a group the heavy metals show less variation than the light. This is further evidence of the insularity of the f-shell when half or more filled. If one assumes a fixed mobility ratio of 0.1 of less, then the large variations in Hall coefficient may be explained by slight changes in N_s. Unfortunately, Anderson reported that he was unable to obtain values of N_s and mobility ratio to give reasonable results consistent with resistivity for all of the metals he studied.

As mentioned previously, the REM's can be described as an assembly of localized trivalent ions imbedded in a sea of itinerant electrons. The dominant coupling between the ions and electrons is through the exchange interaction. (De Gennes 1962) As a result the s-d electrons become

polarized and interact with neighboring ions. Hence the name indirect s-f exchange interaction. The resulting various forms of magnetic order result from variations in the anisotropy energy (Koehler 1965). This is thought to arise from the interaction of the crystalline field with the 4-f electron currents. (Miwa, [1961) 6 693] 1961) Since the hcp structure is anisotropic it is expected that much of the anomalous and unexplained behavior might be due to this. More recently single crystals of most of the REM's have been grown. As a result determination of their magnetic structure was possible of which unexpected complexity was found. Furthermore, their resistivity was found to be highly anisotropic, with the c-axis behavior unusual even for magnetically ordered materials. The a-axis resistivity is normal for magnetic materials. This behavior is reflected in optical properties.

The magnetic structures were found by neutron diffraction in a manner similar to that of x-ray diffraction analysis. (Koehler, [illegible] 1965) Neutrons can reveal the "magnetic lattice" because their intrinsic magnetic moment can interact with the moments of the ions. The magnetic structures of the REM's are summarized in Fig. 1.

Of the lanthanons only Gd easily transforms from the paramagnetic directly to the ferromagnetic state. Also like the similar ferromagnetic transition metals the resistance is composed of two parts. The first is due to the normal phonon-carrier scattering and is proportional to the temperature at high temperatures. The second is characteristic of ferromagnetism. This resistivity is constant above the Curie temperature but drops linearly with temperature becoming zero at $0^{\circ}K$. A small magnetic residual resistance remains due to lattice defects etc. Kasuya

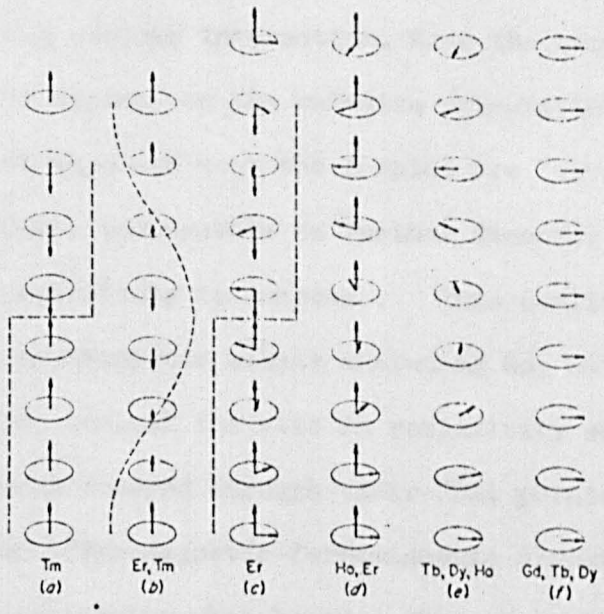

FIG. 1. Schematic representation of magnetic structures of heavy rare-earth metals. The moments are supposed to be parallel in a given hexagonal layer.

Fig. 1 Key:
(a), below 40°K; (b), Er-53.5 - 84°K; Tm-40 - 56°K
(c), 20 - 53.5°K; (d), below 20°K; (e), between T_N and T_C;
(f), below T_C.

1956) and Elliott (1954) first suggested the following model: the f-s exchange interaction (s-d in the transition metals) does not, unlike the coulomb interaction, have the periodicy of the crystal. Instead it depends on the relative orientation of the spins of both electrons. At absolute zero the f-spins are "frozen" into order while above the Curie temperature no further disorder occurs and the magnetic part of the resistivity is constant. This qualitatively explains the normal ferromagnetic metals including Gd, but completely fails to explain the unusual increase in resistivity shown by the antiferromagnetic metals when lowered through their Néel points. Also the metals which have an antiferromagnetic-ferromagnetic transition exhibit a sharp reduction in resistivity when lowered through their Curie temperatures. As seen from the previous figure the s-f interaction results in various oscillatory orderings of the magnetic moments in the hexagonal layers. Since they do not have the same period as the lattice Miwa (1963) and Mackintosh (1962) suggested that forbidden or band gaps are created. The creation of these gaps reduces the conductivity by decreasing the effective number of carriers. Thermally caused magnetic fluctuations also increase the resistivity in like manner to that of ferromagnetic scattering. This quite plausibly explains the behavior of for example erbium. The figure below shows the a- and c-axis' resistivity as a function of temperature (Green, 1961). Superimposed is Miwa's predicted curve.

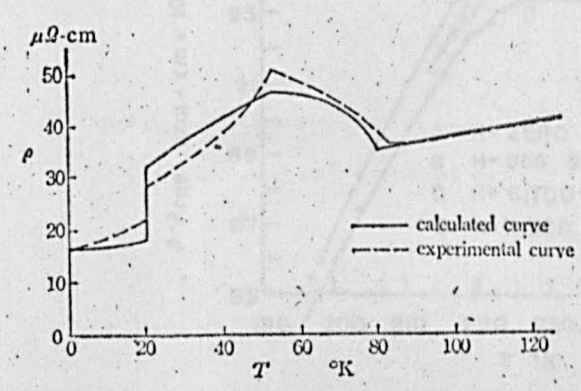

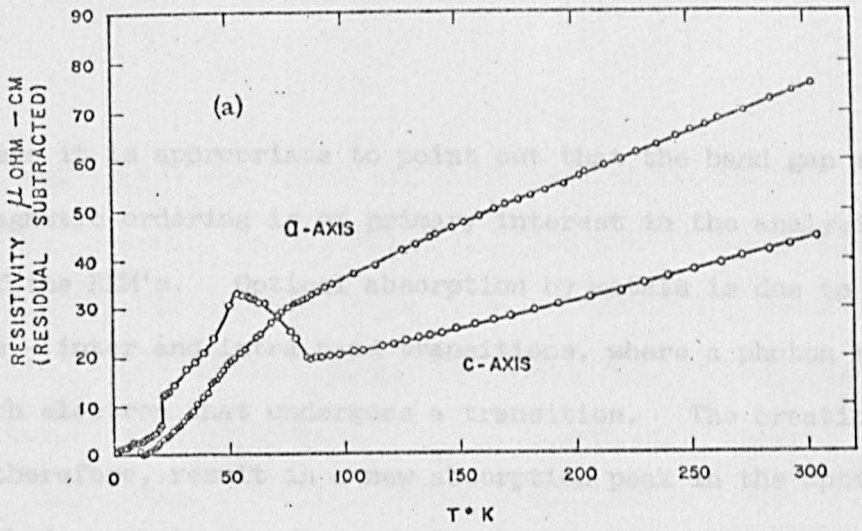

Erbium Resistivity

According to his model at T_N (85°K) the band gaps are created and the resistivity increases as $(T_N-T)^{1/2}$ while the spin-disorder scattering decreases proportionally to T_N-T. Therefore, there is a sharp rise in resistivity. At 53.5° Er undergoes a change in ordering in which the antiferromagnetic order is more comensurate with the lattice. Finally at T_C (20°K) the gaps decrease with the creation of a ferromagnetic moment, with a concomitant sharp increase in conductivity. Terbium exhibits similar behavior and furthermore an 11.35 kOersted field will quench the antiferromagnetic order causing ferromagnetic order above T_C (221°K) and below T_N (229°K). As expected the antiferromagnetic resistivity "bump" is removed and the curve is similar to that of Gd. See the figure below. (Mackintosh, 1962).

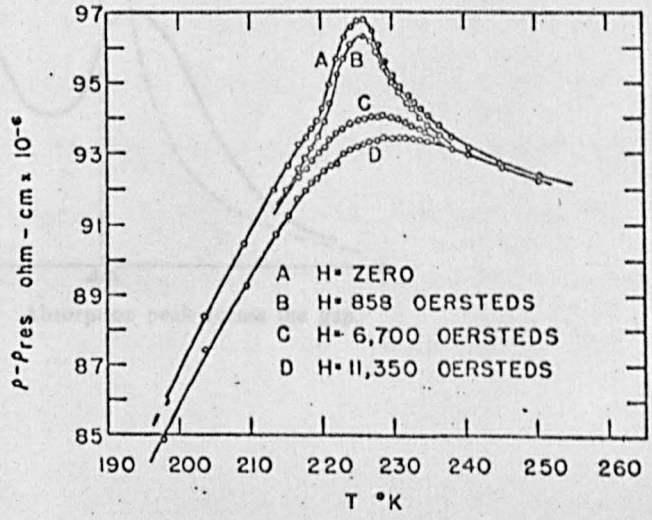

Here it is appropriate to point out that the band gap model with anti-ferromagnetic ordering is of primary interest in the analysis of optical data of the REM's. Optical absorption by metals is due to two principal sources - inter and intra band transitions, where a photon is annihilated for each electron that undergoes a transition. The creation of a new band will, therefore, result in a new absorption peak in the optical conductivity. The dashed curve in the figure below shows the expected absorption caused by a particular band gap with no other effects. However, electron scattering (impurity, phonon electron-electron, lattice defect, and spin disorder) will smooth out the discontinuity at Δ/h, where Δ is the effective magnitude of the energy gap. Actually there may be a series of gap pairs which further complicates the analysis. We have assumed that the new gaps are within the conduction band (since they effect resistivity changes). Therefore, the peak will appear on the intra-band absorption curve. Assuming a Drude form for the intra-band absorption, the absorption will be as shown by the solid line. (Miwa 1963, p.485)

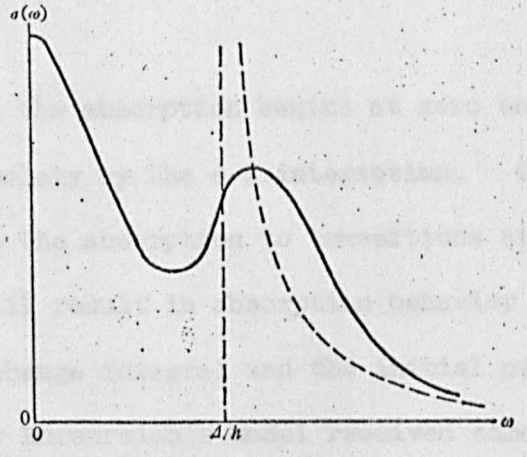

Absorption peak across the gap.

While the dotted line gives the absorption above the Néel point. Unfortunately, however, it has been found that all of the measured REM's that have any type of magnetic order have new absorption bands in the ordered state. (Ho-Schüler, 1964; Dy and Gd - Schüler-Abeles, 1966; Dy - Cooper, 1965, and Tb this work). Furthermore, when a magnetic field above a critical value is applied to a spin ordered metal the ordering becomes ferromagnetic, and the new absorption bands should be removed. A 22 kG field was applied to polycrystalline Dy (H_c = 5 kG at 123°K) and no change was found (Cooper, 1965). Therefore, one must conclude that these new absorption bands in the REM's are characteristic of magnetic order and not of the particular type. Cooper and Redington (1965) suggest an alternate cause that is qualitatively confirmed in this work. They point out that from theoretical work the REM's like nickel have a d-like conduction band i.e. flat with a high density of states at the Fermi level, and, therefore, might be expected to behave in a similar fashion. This d-like nature is certainly verified experimentally by their high electronic specific heat. Ehrenreich (1963) was able to find transitions at symmetry points from spin split bands which explained the new absorption in Ni.

In Miwa's model the absorption begins at zero energy and moves to a value determined solely by the s-f interaction. On the other hand a model which ascribes the absorption to transitions created by the splitting of existing bands will result in absorption behavior that depends upon the magnitude of the exchange integral and the initial position of the band in question. Recently Ehrenreich's model received some additional confirmation by Shiga and Pells (1969). They found that the absorption at 1.4 eV is

reduced in value with increasing temperature. However, the position of the peak does not change with temperature and a trace of it remains above the Curie temperature to 770°K (Curie temp. 630°K). On the other hand the main peak (4.7 eV, Curie temp.) position moves linearly to lower energy with temperature both above and below the Curie temperature, (4.4×10^{-4} eV/C°). It, however, consists of two unresolved peaks in the ordered state, as its width decreases with temperature below the Curie temperature (.2 eV, -17%, 77°K to 630). In fact the change in width is proportional to the spontaneous magnetization.

One of the motivations for the study of optical properties of the REM's has been to find evidence of 4-f - 4-f transitions which give so profuse an absorption spectrum in the visible from RE salts. Both Kern (1957), aTannhäuser (1962), and Schüler (1966) looked for these lines in their absorption data of the metals. Kern explained their absence from his data to be due to the lack of differential sensitivity in his measurement for k (absorption coefficient). He assumed that the oscillator strength (f) for the transition were no greater in the metal than in the salts. A similar result obtains for this work and will be shown later.

CHAPTER 1

ELECTROMAGNETIC AND ELLIPSOMETER THEORY

The optical properties of a material for low intensity radiation are completely described by two constants, n and k, the index of refraction and the extinction coefficient. In general they are actually frequency dependent tensors, however, for isotropic or polycrystalline media they reduce to scalar functions. As the metals studied are assumed to be randomly oriented polycrystalline films n and k will be treated as scalar.

The origin and meaning of the optical constants is found in Maxwell's equations. It is easily shown that if either $\underline{E}$ or $\underline{B}$ is eliminated from Maxwell's equations the result is a pair of wave equations of the form:

Eq. 1 $$\nabla^2 \underline{E} = \frac{1}{V^2} \ddot{\underline{E}} + G \dot{\underline{E}}$$

electric field case where $V \equiv (\mu\mu_0 \varepsilon\varepsilon_0)^{-1/2}$ and $G \equiv \mu\mu_0\sigma$ μ_0 & ε_0 are the free space permeability and permitivity; μ & ε the relative permeability and permitivity and σ the conductivity.

If one assumes a plane wave solution represented by the real part of:

Eq. 2 $$\tilde{A} \exp(i \tilde{\underline{K}} \cdot \underline{R} - i\omega t)$$

where $\tilde{\underline{K}} = K_1 + i K_2$, $K_1 = n\omega/c$ & $K_2 = k\omega/c$ $\left\{ \begin{array}{r} \mu_0 \equiv 4\pi 10^{-7}\ H/m \\ c = (\mu_0\varepsilon_0)^{-1/2},\ \varepsilon_0 \equiv 10^7/4\pi c^2\ F/m \end{array} \right\}$

then n and k are required to be unique functions of the conductivity and permitivity of the medium. They are on substitution:

Eq. 3 $$K_1^2 - K_2^2 = \omega^2/V^2 \text{ , \& } K_1 K_2 = G\omega/2$$

or Eq. 4 $$n^2 - k^2 = \mu\varepsilon \text{ , \& } 2nk = \frac{\sigma\mu}{\omega\varepsilon_0} \text{ , or } nk/\lambda = \frac{\sigma\mu}{c\varepsilon_0 4\pi}$$

The function nk/λ is equal to $30\sigma_{dc}(\omega=0)$ and, therefore, homologous to the d.c. conductivity of a material. As required, as $\omega \to 0$ nk/λ_0 approaches the d.c. value.

In Eq. 2, $\tilde{K}$ is the complex propagation vector. The real part contains the velocity function, n, which is perpendicular to the planes of constant phase. While the imaginary part contains the absorption function, k, which is perpendicular to the planes of constant amplitude. Usually these vectors are parallel (homogenous waves). An inhomogenous wave may be produced by passing a plane polarized wave through an absorbing prism, thereby producing a wave with a component of K_2 transverse.

n and k are found by experiment while ϵ and σ may be found from theoretical models described in Chapter 2.

The measurement of n and k make use of reflection coefficients applied to plane polarized light. When such light is reflected by a metal it becomes elliptically polarized because the phase change on reflection is other than zero or pi for the components. In the presence of absorption the relative phase difference, $\Delta = \delta_p - \delta_s$, between the components parallel and perpendicular to the plane of incidence is zero and pi only when the angle of incidence, φ, is pi/2 and zero. At a particular angle of incidence, $\bar{\varphi}$, Δ = pi/2. At this angle, $\bar{\varphi}$ and Δ, and the ratio of the reflected components are most sensitive to variation of n and k. Known as the principle angle of incidence it corresponds to Brewster's angle for dielectrics where Δ changes discontinuously by pi.*

---

* Note: The principle angle of incidence usually differs by a fraction of a degree from the pseudo-Brewster's angle, where r_p is a minimum.

The reflection coefficients are derived from boundary conditions required by Maxwell's equations. The boundary is usually assumed discontinuous, for uncontaminated and sharply defined (polished) surfaces this is a good approximation for wavelengths long compared to atomic dimensions. However, the breakdown of Fresnel's equations at the Brewster's angle of glass due to a transition layer is easily found, as an ellipticity other than zero is easily detected. A number of authors have reported deviations from zero which upon cleaning and/or polishing was reduced (Hodgson, 1967). A quantitative treatment given by Drude shows that a transition layer of smoothly varying intermediate index of refraction will result in the ellipticities found. In fact the theory predicts that a layer of non intermediate index can result in a negative ellipticity. This is found for glass with a grease layer. Typical transition thicknesses are of the order of 10^{-9} m. This error, however, is minor compared to the effect of oxide layers formed on metals exposed to air. For example the reflectivity (intensity) at normal incidence of iron is reduced from 0.49 to 0.44 (10%) by a layer of its oxide 7×10^{-9} m thick, (Hodgson, 1967). For iron at an O_2 partial pressure of 10^{-5} torr, a 10^{-9} m thick oxide layer is formed in approximately half an hour. Since even the least reactive of the rare earths undoubtedly has a sticking probability greater than that of iron (5×10^{-3}) (Kruger, 1964), it is necessary that preparation and measurement be made at a pressure well below 10^{-5} torr.

Assuming the absence of a transition layer the optical constants can be uniquely calculated from the geometry of the ellipse of the reflected wave. That elliptical polarization results and how the parameters of the

ellipse are used to determine the optical constants is now shown.

The simplest method of analysis is to assume an incident beam with a linear polarization of 45° with respect to the plane of incidence. This may be represented by:

Eq. 5

$$E_x = r_s \cos(\Upsilon + \delta_s)$$

$$E_y = r_p \cos(\Upsilon + \delta_p)$$

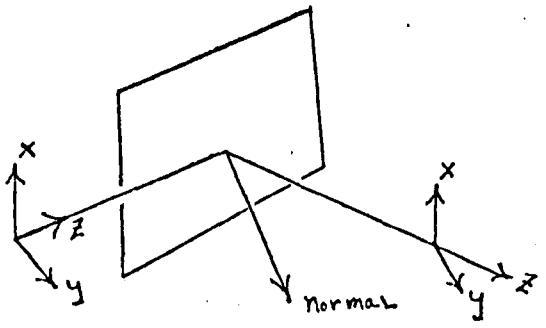

z is in the direction of propagation and $\Upsilon = (\omega\tau - \tilde{K}\cdot R)$ with $r_p = r_s$, $\delta_p = \delta_s$. Upon refelection r'_p and r'_s will usually differ as will the phases δ'_p and δ'_s. As only the difference $\Delta = \delta'_p - \delta'_s$ is relevant δ'_s may be set to zero. Therefore, eliminating τ from equation (5) one obtains:[1]

Eq. 6 $$\left(\frac{E_x}{r_s}\right)^2 + \left(\frac{E_y}{r_p}\right)^2 - 2\,\frac{E_x E_y}{r_s r_p}\cos\Delta = \sin^2\Delta$$

the equation of an ellipse centered at the origin with arbitrary rotation of its axis. The ratio of the reflection coefficients are a function of Δ and the ratio of r_p and r_s, which must now be found from the ellipse. However, the ratio, (r_p/r_s), is easily found by measuring the intensities in the s and p directions with a linear detector and an appropriately oriented analyser.

To find Δ the angles ψ and η must be defined. ψ is equal to the arc tangent of the amplitude ratio of the p and s reflected waves; while η is the arc tangent of the amplitude ratio of the minimum and maximum values

[1] Primes now dropped.

of the reflected wave; i.e., the ratio of the semi-axis' of the reflection ellipse. The significance of ψ and η is evident if equation (6) is transformed by the substitution: $r_s = c\cos\psi$, $r_p = c\sin\psi$ (which implies $r_p/r_s = \tan\psi$ and $r_s^2 + r_p^2 = c^2$)

Equation (6) then becomes:

Eq. 6a $$E_x^2 \tan^2\psi + E_y^2 - 2E_xE_y\tan\psi\cos\Delta = c^2\sin^2\psi\sin^2\Delta$$

and the resulting ellipse may be inscribed in a rectangle of sides $2r_s$, $2r_p$, and diagonal 2c. ψ then is the angle formed by c and r_s.

To find Δ one rotates the ellipse by an angle γ with the Cartesian rotation transform so that the axes' of the ellipse are coincident with the coordinant axes. The term in xy is zero if:

Eq. 7 $$\tan 2\gamma \equiv \tan 2\psi\cos\Delta$$

Now ψ and Δ are known and with the angle of incidence, φ, the optical constants may be found from the reflection coefficients. However, ψ and Δ may be found independently of a direct measurement of the s and p waves. If the further substitution

Eq. 8 $$\sin 2\eta = \sin 2\psi\sin\Delta$$

is performed equation (6a) reduces to:

Eq. 6b $$\frac{X'^2}{c^2\sin^2\eta} + \frac{Y'^2}{c^2\cos^2\eta} = 1 \quad \text{or} \quad \frac{X^2}{b^2} + \frac{Y^2}{a^2} = 1$$

where a and b are the major and minor axes of the ellipse.

From equations (7) and (8) one may obtain:

Eq. 9 a $$\cos 2\psi = \cos 2\eta\cos 2\gamma$$

b $$\tan\Delta = \tan 2\eta\ \mathrm{cosec}\, 2\gamma$$

Therefore, only one angular and two intensity measurements are necessary to determine the ellipse parameters ψ and Δ. However, the amplitude measurement of the s and p waves may serve as a check or may be used instead of equation (9a) to simplify calculations. Now that Δ and ψ are known the optical constants may be found through Snell's law and the appropriate Fresnel equations. For absorbing media Snell's law implies that the angle of refraction, (χ), is complex:

Eq. 10 $$\sin\Phi = N \sin\chi \qquad N \equiv n + ik$$

as Φ is the real angle of incidence. Using the initial conditions and definitions of equation (5), the ratio of the reflected amplitudes, (ρ), will be:

Eq. 11 $$-\rho e^{i\Delta} = \cos(\Phi+\chi)/\cos(\Phi-\chi)$$

or by the definition of the angle ψ:

Eq. 11b $$-\tan\psi\, e^{i\Delta} = \cos(\Phi+\chi)/\cos(\Phi-\chi)$$

Eliminating χ by substituting equation (10) one obtains:

Eq. 12 $$N^2 = \left(\frac{1-e^{i\Delta}\tan\psi}{1+e^{i\Delta}\tan\psi}\right)^2 \sin^2\Phi\tan^2\Phi + \sin^2\Phi$$

To be useful equation (12) must be reduced to the form: $N^2 = A + iB$. Two forms are known: due to Drude and Price. Drude's equation is of simpler form but is computationally lengthy. Price's (Price, 1946) is suitable for a series of measurements at various wavelengths with fixed angle of incidence. The result is:

$$A = \tan^2\Phi - \left[\frac{2\sin^2\Phi\tan^2\Phi(\cos\Delta+\sin 2\psi)}{\sin 2\psi(\cos\Delta+\operatorname{cosec} 2\psi)}\right]$$

Eq. Eq. 13

$$B = 2\sin^2\Phi\tan^2\Phi\sin\Delta / \tan 2\psi(\cos\Delta+\operatorname{cosec} 2\psi)^2$$

In practice the metal being measured is deposited upon the rear face of a silica glass prism whose angle is equal to the desired angle* of incidence, therefore, N^2 is multiplied by the square of silica's index of refraction at the particular wavelength being used. Furthermore, as will be presently shown, interchange of the analyser and polarizer does not change the intensity of the light leaving the second polarizer if the light entering the first is unpolarized. This is fortunate as monochrometers polarize light, while many common light sources emit unpolarized light. Given the previously stated requirement, for a polarizer with azimuth ψ_{Pol} the p and s amplitude components reflected by a specimen will be (Conn, 1954):

$$A_o r_p \cos\psi_{pol} \cos(\omega t+\delta_p), \text{ and } A_o r_s \sin\psi_{pol} \cos(\omega t+\delta_s)$$

where A_0 is the amplitude of the incident wave with angular frequency ω, r_p and r_s are the reflection coefficients of the specimen and δ_p and δ_s the reflection introduced phase changes.

The amplitude transmitted by the analyser of azimuth ψ_A will then be:

$$A_o r_p \cos\psi_{pol} \cos\psi_A \cos(\omega t+\delta_p) + A_o r_s \sin\psi_{pol} \sin\psi_A \cos(\omega t+\delta_s)$$

The intensity, therefore, is:

$$\text{Eq. 14} \quad I = A_o^2\left[|r_p|^2\cos^2\psi_{pol}\cos^2\psi_A + |r_s|^2\sin^2\psi_{pol}\sin^2\psi_A + \tfrac{1}{2} r_p r_s \sin 2\psi_{pol}\sin 2\psi_A \cos\Delta\right]$$

where $\Delta = \delta_p - \delta_s$

As the intensity function is symmetrical in ψ_A and ψ_{Pol} the two polarizers' function may be interchanged, thereby the necessity for a diffusion screen with its intensity reduction is removed.

---

*To prevent refraction and change in polarization.

Several other methods of measuring optical constants are commonly used, but it is felt that they in general suffer from inconveniences or lack of precision. Fig. 1.1 illustrates the various ellipsometric parameters.

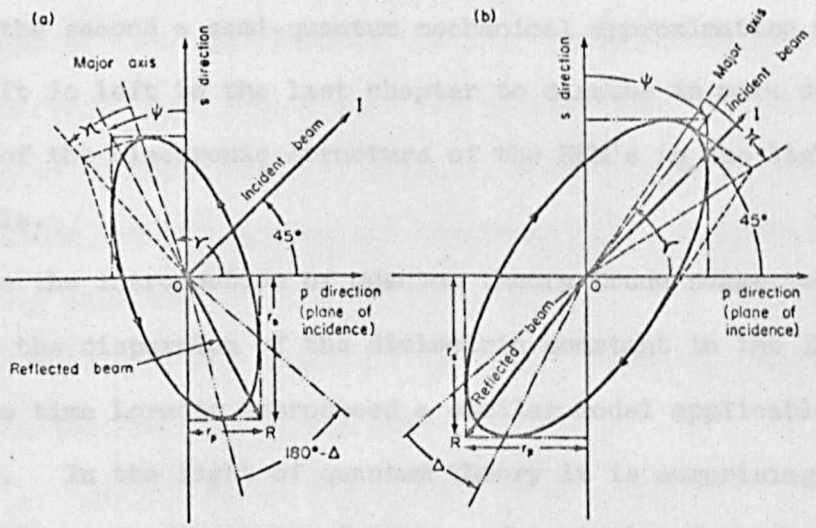

Fig. 1.1 Graphical representation of various ellipsometric parameters for (a) reflection at an angle of incidence less than the principal angle, and (b) one greater than the principal angle.

CHAPTER 2

THEORY

It is through the use of models that an interpretation of optical data may be made to give a microscopic electronic description of solids. In this chapter two models will be described and the general optical character of metals will be related to them. The first is a classical model and the second a semi-quantum mechanical approximation using band theory. It is left to the last chapter to discuss in more detail the character of the electronic structure of the REM's in the light of these models.

Before the introduction of quantum theory Drude suggested a model to explain the dispersion of the dielectric constant in the IR for metals. At the same time Lorentz introduced a similar model applicable to insulators. In the light of quantum theory it is surprising that such a naive model gives dispersion formulae of a similar form to that derived from perturbation and band theory. Since these formulae give valuable insight and a simple means of relating optical data they will be described. Since the complex dielectric constant, $(\tilde{N}^2)$, relates to the absorption and phase shift of waves in a physical system, certain boundary conditions (a result of causality), are observed. Therefore, integral relations between the dielectric constant, (n^2-k^2), and the conductivity (nk/λ), obtain, independent of the form of the dispersion. They and others of a similar nature have been named Kramers-Kronig relations because of their original work. Also from the high frequency limit of the Drude-Lorentz formula and a K_0-K_0 relation a useful sum rule will be derived.

In the Lorentz theory optical absorption bands result from the excitation of "Lossey" electron oscillators. The oscillators are electrons bound to nuclei by a linear restoring force. In order for the oscillators to absorb energy linear damping is introduced. This model gives an equation of motion with three phenomenological parameters. One is the mass of the electron; the restoring force and the mass determine the oscillator frequency. Finally the damping constant which is an attempt to take into account the scattering processes which restore the oscillators to equilibrium when the driving force is removed. A single term to encompass lattice effects, phonon, and electron interactions etc. is a gross simplification, but the result is quite meaningful and qualitatively accurate.

If the effective and applied field is, F = real $\tilde{F}_0 \exp(-i\omega t)$, then the equation for the motion of $\tilde{X}$ is:

Eq. 2.1 $$m^*\ddot{\tilde{x}} + m^*\omega_c\dot{\tilde{x}} + m^*\omega_o^2\tilde{x} = eF_o\exp(-i\omega t)$$

where m* is the "effective" mass of the electron. The second term is the damping including the phenomenological damping constant ω_c. The third term is the linear restoring force. The solution given by a number of authors (for example, Moss 1959) is

Eq. 2.2 $$\varepsilon_1 \equiv n^2 - k^2 = \frac{\omega_p^2(\omega_o^2-\omega^2)}{(\omega_o^2-\omega^2)^2+\omega^2\omega_c^2} + 1$$

$$\varepsilon_2 \equiv 2nk = \frac{\omega_p^2\,\omega\,\omega_c}{\omega_o^2-\omega^2}$$

where $\omega_p = [N_v e^2/m^*\epsilon_0]^{1/2}$ (mks)

ω_p is the plasma resonance frequency whose significance will be discussed later. N_v is the electron concentration, e the electronic charge, and ϵ_0 the permittivity of free space ($8.854\ 10^{-12}$ Fd/m). The behavior of ϵ_1 and ϵ_2 is shown in Figure 2.1c.

If the electrons are quasi-free, ω_0 is zero, and the equations are:

Eq. 2.3 $$\epsilon_1 = 1 - \omega_p^2/(\omega^2+\omega_c^2)$$

$$\epsilon_2 = \frac{\omega_p^2 \omega_c}{\omega(\omega^2+\omega_c^2)}$$

From the Drude theory of metallic conduction $\sigma_{DC} = e^2 \tau N_v/m^*$(cgs) where τ is the time between collisions and is approximately equal to the inverse of ω_c. Therefore, from the definition of optical conductivity the imaginary part of the solution may be written

$$\sigma = \frac{\sigma_{DC}}{1+\left(\frac{\hbar\omega}{\hbar\omega_c}\right)^2}$$

where σ_{DC} is the limit of the optical conductivity in the IR and $\hbar\omega$ is the photon energy. If it is measured in eV's then $\hbar\omega_c$ is seen to represent the damping frequency at which σ falls to 1/2 of σ_{DC}. This behavior is shown in Fig. 2.1a and d.

The significance of the definition $\omega_p^2 = N_V e^2/m^*\epsilon_0$ may be seen if in Eq. 2.1 the right hand member is a linear coulomb restoring force $-\tilde{X}N_V e^2/\epsilon_0$. This corresponds to a plasma where X is the separation of the charges. The solution is $\tilde{\omega} = \omega_p - i\omega_c/2$. If ω_c is small, i.e. $\epsilon_2 \to 0$, then ω_p is seen to be the natural frequency of a collection of "free" undamped

electrons in a metal (plasma). Hence the term. The plasma oscillation is a longitudinal wave which must be excited by a longitudinal field. The existence of such a wave follows from Maxwell's equation $\nabla \cdot 0 = 0$ (Hodgson, 1970). Such a field may be excited by an obliquely incident p wave.

Electron probes also excite plasma oscillations in addition to one electron excitations. It can be shown that the energy loss from such a probe is proportional to the product of ω and the imaginary part of the inverse of the dielectric constant. The fact that very good agreement is found for the dielectric constants found by optical and electron probes confirms the prediction of the one electron or random phase approximation that the longitudinal and transverse constants are equal at optical frequencies. Fig. 2.1d shows the behavior of ϵ_1, ϵ_2 and $\mathrm{Im}(1/\tilde{\epsilon})$ where properties are dominated by free electrons.

The K-K transform (Frank Stern 1963, Landau and Lifshitz 1963, J. N. Hodgson 1970)

Eq. 2.4 $$\varepsilon_{1(\omega_0)} - 1 = \frac{2}{\pi} \int_0^\infty \frac{\omega \varepsilon_2 \, d\omega}{\omega^2 - \omega_0^2}$$

is useful, as it affords a means of checking the internal consistency of optical data. The computationally more convenient form used is obtained by transforming Eq. 2.4 to a logarithmic frequency scale (Hodgson 1962).

Eq. 2.5 $$\varepsilon_{1(J_0)} = \frac{2h}{\exp(Jh)} \sum_{J=0} \frac{\sigma_{(J_0+J)} - \sigma_{(J_0-J)}}{\sinh(Jh)} + 1$$

The integral has been written as a sum for numerical integration, h is the width of the sector and $J = \mathrm{Ln}(1/\lambda)$.

Above the plasma frequency, (ω_p), all but the core electrons behave

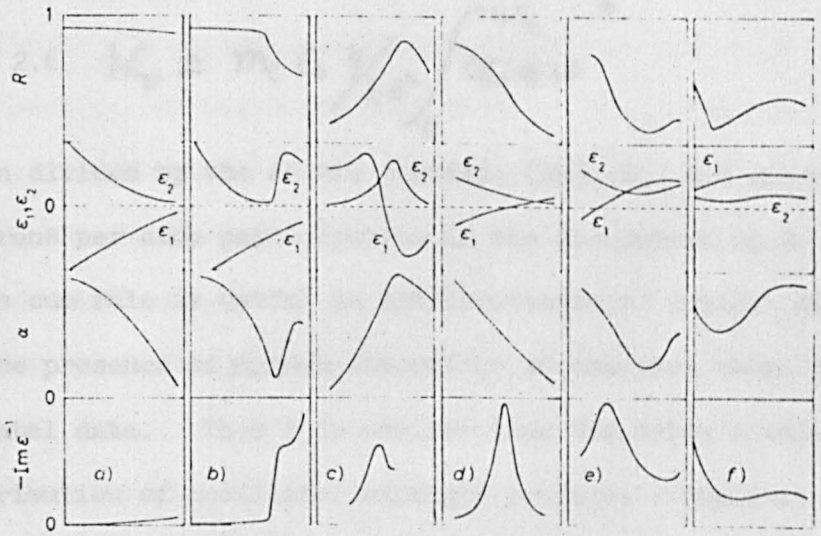

Fig. 2.1 – Typical behavior of optical constants associated with various excitation processes in metals and insulators: metals: *a*) free-electron range, *b*) low-energy interband transitions; semiconductors or metals: *c*) interband transitions, *d*) plasma region, *e*) plasma region modified by interband transitions, *f*) excitation of deeper bands above plasma frequency.

as free particles. (That is with little damping and free mass.) Therefore, $\epsilon_1 = 1 - \omega_p^2/\omega^2$. When Eq. 2.4 is rewritten as

$$\epsilon_1(\omega_0) = 1 - \frac{2}{\pi\omega_0^2}\int_0^{\infty} \frac{\omega\epsilon_2(\omega)\,d\omega}{1 - \omega^2/\omega_0^2}$$

it is seen that as long as $\omega_0 \gg \omega_u \geq \omega$ the upper limit may be ω_u and ϵ_1 replaced by $1 - \omega_p^2/\omega^2$. Thus $\omega_p^2 = \frac{2}{\pi}\int_0^{\omega_u} \omega\epsilon_2(\omega)\,d\omega$, or

$$\text{Eq. 2.6} \quad N_v = m_e\epsilon_0 \frac{2}{\pi e^2}\int_0^{\omega_u} \sigma(\omega)\,d\omega$$

When divided by the atomic density, (Na), Eq. 2.6 gives the number of electrons per atom participation in the absorption up to ω_u, (f).

This sum rule is useful in interpretation of optical data, as it may reveal the presence of further absorption at energies above that of experimental data. Then f is smaller than the metal's valence. Also the distribution of oscillator strength provides a qualitative measure of band mixing.

Several characteristics of the preceding dispersion relation merit mention as they pertain to their application. As is expected intuitively, the hyperbolic sine in the denominator is a weighting function causing the value of the integral to be insensitive to σ far from ω_0. Also σ used for evaluation of ϵ_1 can differ by a constant from the "correct" values without affecting the result. $\sigma(\omega_0+\delta) - \sigma(\omega_0-\delta)$ on a logarithmic scale is in effect the derivative of $\sigma(\omega)$.

As a result, depending on the details of the computation, rather good success can be obtained with limited and unreliable data especially in the case of dielectrics with a limited number of absorption bands. However, with metals a very significant part of the absorption may be in

the infrared beyond the limits of the experimental data. Fortunately this region is often accurately described by the Drude expression in which only two constants must be determined. One, the conductivity at zero frequency, is simply 30 times the D-C conductivity, and therefore fixed. The other ω_c can be found either by fitting to the data or using a value which gives the best ϵ_1 values. At the other end of the spectrum more difficulty is encountered especially if the optically active electrons have not been nearly accounted for by use of the f sum rule. As the reader has probably surmised the transform under discussion has limited usefulness beyond checking of internal consistency of experimental data. Any optical experiment which yields σ must also give ϵ_1. However, as illustrated the transform does serve as a check on extrapolations.[1]

Of more direct use in determination of optical constants are the relations connecting n and k and Ln r and and θ_r. They are:

$$n_{(\omega_0)} - 1 = \frac{2}{\pi}\int_0^\infty \frac{\omega k(\omega)\, d\omega}{\omega^2 - \omega_0^2}, \quad \theta_{r(\omega_0)} - \pi = -2\omega_0/\pi \int_0^\infty \frac{\mathrm{Ln}\, r_{(\omega)}/r_{(\omega_0)}\, d\omega}{\omega^2 - \omega_0^2}$$

the inverse relations are less often used.

where n, k have been previously defined and Ln r and θ_r, (the logarithm of the amplitude of reflectance and reflectance phase, respectively), are the real and imaginary parts of the logarithm of reflectance. Only one measurement of the direct and reflected (at normal incidence) beam are necessary to determine r.

---

[1] Note that the transform is not sensitive to the exact shape of the extrapolation. Radially different extrapolations have been found to give "correct" ϵ_1 values. Fortunately use of "extreme" extrapolation may be eliminated by other considerations.

Once θ has been found from the transform of r, the relations:

$$n = (1-r^2)/(1+r^2-2r\cos\theta)$$

$$k = 2r\sin\theta/(1+r^2-2r\cos\theta)$$

yield the constants. A number of authors report good results from this method except at low values of r. In this region the other relation is useful as k is small enough to be determined by measurement of the absorptions by two thicknesses of the material. However, care must be exercised as films thinner than $2\text{-}3\ 10^{-8}$m often do not exhibit bulk properties.

The classical model, of course, does not give a true microscopic description of electronic behaviour. It suffers, for example, from the defects of not predicting the intensity or position of absorption bands. Further, the loss mechanism is not given - its effect is just simply incorporated with the aid of the parameter, ω_c. The problem of an electronic description of crystalline solids and their interaction wit light is in principle "solved" by quantum theory. Unfortunately this is a many body problem and, therefore, simplifying approximations must be made. The one most commonly used treats the interaction as being with a single electron existing in a self consistent field due to all the ot ers. This interaction is then combined with a knowledge of the electron states to give the dielectric constant. The interaction is given by the transition probability: (Harbeke, 1972)

$$\text{Eq. 2.7} \qquad \omega_{ou} = \frac{he^2E_o^{\,2}}{2\pi^2m_e^{\,2}\omega^2}\int dK\ |\hat{E}.M_{ou}|^2\delta(E_u-E_o-h\omega)$$

where E_o is the electric field, and $\hat{E}$ is the polarization vector of the electric field. $|\hat{E}.M|$ is the matrix element

$$\int_V dr\ \exp\left[-i(K_u-k).r\right]\ U_u^*\ \hat{E}.\nabla\ \exp\left[iK_o.\gamma\right]u_o$$

The upper case K's refer to the electronic wave functions and k to the

vector of the radiation. The U's are the lattice modulating functions which are translationally invariant. The orthogonality of the Bloch functions gives the direct transition selection rule. The integral vanishes unless $K_U - k = K_0 + G$ where G is any reciprocal lattice vector. $|k|$ is small compared to the width of the Brillouin Zone, therefore, in the first B.Z. $K_U = K_0$. The momentum is conserved and transitions are vertical. Non-vertical transitions are possible if the difference in momentum is furnished by a phonon. The δ function gives the second selection rule requiring that the photon supply the difference in energy between the final and initial electron states. In indirect transitions the selection rule is: $\delta(E_U - E_0 - \hbar\omega \pm E_{(q)})$. ω_{ou} is easily related to the conductivity since by definition $\omega_{ou}\hbar\omega$ is the energy gained by the crystal while Maxwell's theory gives $1/2\ \sigma|E|^2$ as the incident wave's energy loss. Therefore, the conductivity is

Eq. 2.8 $$\sigma_{ou} = \frac{\pi e^2}{2\pi^2 m_e \omega} \int_V d\underline{K} \left|\hat{E}\cdot M_{ou}\right|^2 \delta(E_u - E_o - \hbar\omega)$$

The conductivity for a given ω is then the sum of all transitions between occupied and unoccupied states with a ΔE of $\hbar\omega$ weighted by the square of the matrix element. By using the properties of the δ function the K space integral may be transformed into an integral over the surface $E_0(K) - E_u(K) = \hbar\omega$.

Eq. 2.9 $$\sigma_{ou} = \frac{\hbar^2 e^2}{\pi^2 m_e^2 \omega} \int_S \frac{dS\left|\hat{E}\cdot M_{ou}\right|^2}{\left|\nabla_K (E_u - E_o)\right|_{E_u - E_o = \hbar\omega}}$$

Direct calculations on many possible cases indicate that in general the matrix element varies slowly with ω so that the shape of σ is dominated by the joint density of states given by Eq. 2.10

Eq. 2.10 $$J_{ou}(\omega) = \int_S \frac{dS}{|\nabla(E_u - E_o)|_{E_u - E_o = \hbar\omega}}$$

J has critical points at symmetry points and lines where the energy bands have maxima, minima, or saddle points. J also may peak where only the difference of the gradients is zero.

Since ellipsometrically measured σ does not differentiate between different band pairs matrix element selection rules should be incorporated in any attempt to compare σ data and density of state calculations. The non conservation of parity is the principal selection rule. Parity is a good quantum number for Bloch functions at the center of the BZ, and at some of the symmetry points of the BZ faces. At other points parity is not good, but if a transition is forbidden at a symmetry point it is unlikely that nearby the matrix element will reach a high value. Ideally one would prefer to find the convolution of a density of states calculation for the whole BZ and then delete the portions due to forbidden transitions. Probably because of the high electron density, it was found that a number of transitions forbidden by symmetry either must be permitted in order to obtain good agreement with experiment, or transitions from the volume of the BZ dominate the conductivity. This is especially evident in Fig. 5.1 where all of the transitions for Gd at 1.5 ev are forbidden by symmetry. On the other hand some peaks in σ are predicted by J but are absent in the data. This is discussed in the last chapter. In order to estimate the

volume contribution Endriz and Spicer (1970) indicate the number of equivalent points and faces in a plot of energy differences between occupied and unoccupied bands. This was noted when some of the tabulations of direct transitions were made for the last chapter, but did not result in significant changes in the histograms. Both simple convolutions of density of state histograms and histograms of direct transitions were done for the comparisons in the last chapter.

CHAPTER 3

EXPERIMENT

As stressed in Chapter 1, the lanthanides demand rather stringent preparation conditions in order to obtain surfaces that are characteristic of the interior of pure bulk metal. These requirements exist to some extent for all metals with the possible exception of the noble metals. Therefore, the apparatus, while constructed by Dr. J. N. Hodgson for the preparation and measurement of other metals, was successfully used for the lanthanides.

Three possible solutions to the preparation problem have been used. The most common is to deposit in very high vacuum, $< 10^{-9}$ torr, films which are then immediately measured *in situ* or, having been deposited on a window in an ampoule or cell, are sealed off and placed in the measurement apparatus. A second obvious method is to polish bulk metal, then preserve it until it is placed in a vacuum or inert atmosphere cell. The latter was used by Knyazev *et al.* on Gd, Sm and Dy. The last method, used to obtain the present results, is to deposit a rather thick film on a face of a prism (silica). The metal surface in contact with the prism is then protected from atmospheric contamination by further metal deposited behind it and the silica in front. A prism is used as the incident and reflected pencil may then be normal to the glass preventing polarization. Eq. (13) of Chapter 1 was derived assuming a vacuum metal interface. Therefore, A and B must be divided by the index of refraction of the prism material. Strain birefringence is still possible, but was not thought to be significant as uncoated prisms gave values of ψ and γ within a few tenths of a degree.

Diffusion pump oil was used to improve the

thermal contact of the prisms when cooled by a liquid nitrogen heat sink. Since it froze, strain might be introduced. It was found to be insignificant on comparison with data taken at slightly higher temperatures with and without the oil using Gd films which were not very sensitive to temperature. Unfortunately, this method was not completely successful with Nd and possibly Yb. That it was with Gd is shown in Fig. 3.1. The elapsed time between the measurements shown is more than a year. The difference ($\sim$ 3%) in the low temperature data may be explained by the variation in temperature. However, there does seem to be a significant difference (4%) in the room temperature data above 2 eV. However, this is less than the difference between different Gd films.

This method almost failed with Nd because it reacts with the silica substrate. (It was necessary to protect the film from atmospheric attack with vacuum grease.)

The films were prepared in a commercial (Varian) VI-5 vacuum system. Varian Ti getters were used in an effort to attain the base pressure ($\sim 10^{-8}$ torr) used more quickly. Often they did not work actually increasing the pressure. Also a copper cold finger (ℓN_2) was sometimes used during deposition. Often it seemed to have no effect.

All the metals were deposited by evaporation from self Joule heated tantalum boats. It was necessary to wrap a strip around the boat when Yb was evaporated. This is because Yb sublimes and the material used generated so much gas when heated that without the strip it was ejected from the boat. Also coated was a spectrosil slide in a four terminal configuration suitable for resistance measurement.

The first photograph shows the substrate holders (another was also used

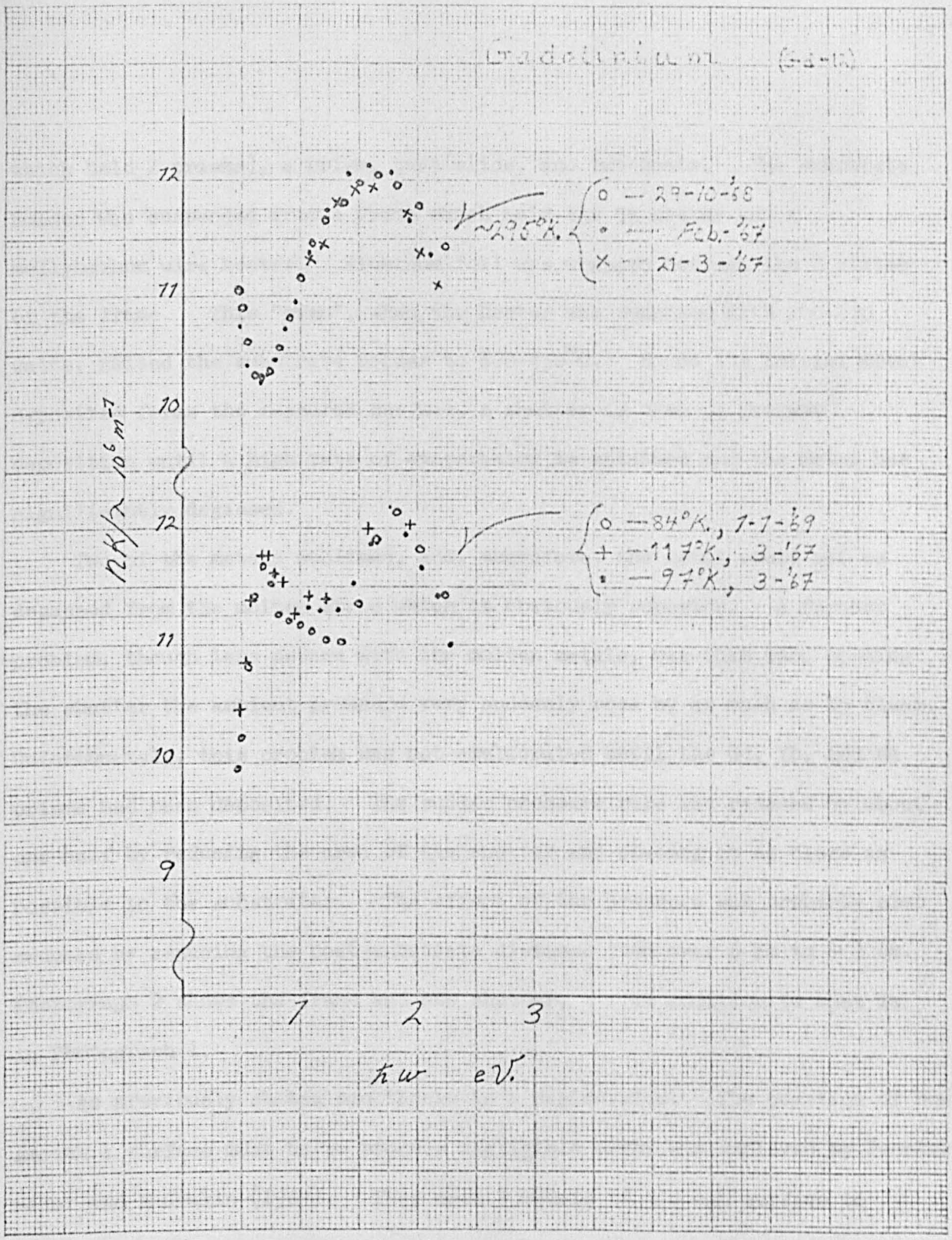

Fig. 3.1 Relative lack of Aging in gadolinium

which held 2 prisms), a prism, test slide, and two boats. The substrate holder was suspended from a frame which held the Ti getter and a mollybdenum wire heater. Aluminum foil was wrapped between the 2 plates of the frame. This "oven", when the heater was supplied with 200-270 watts, raised the substrate holder to 400-450°C. Since the initial metal deposited forms the measured surface, a shutter is used to prevent deposition until a high rate of evaporation is attained and the metal has significantly degassed.

Two of the metals sublimed, and, therefore, the metal could not be degassed from the molten state which is obviously superior. A further problem, though less severe with the molten metals, was that upon opening the shutter the ambient pressure very suddenly rose by as much as 25 times. Unfortunately, this problem was not ameliorated until the Gd, Yb, and Nd prisms had been deposited. The sudden pressure rise was reduced by about one-half by reducing the area of the shutter and placing it as close as possible to the substrates. The effect of the pressure was probably also reduced by reducing the boat-substrate distance from over 6 cm to ~ 3 cm. Photograph 2 shows the frame and new shutter, in addition to what is in Photograph 1.

As previously stated smoothness is a desideratum. The question of how smooth a surface must be to produce negligible error was explored by Fenstermaker and McCrakin (1969). They used 3 models of a rough surface to theoretically determine the error caused by roughness on the optical constants of 6 materials measured ellipsometrically. They found that a surface roughness of 10 Å could cause changes in n and k of 0.01 to 0.1 in n and as much as 0.28 in k. Vacuum deposited metals contour their sub-

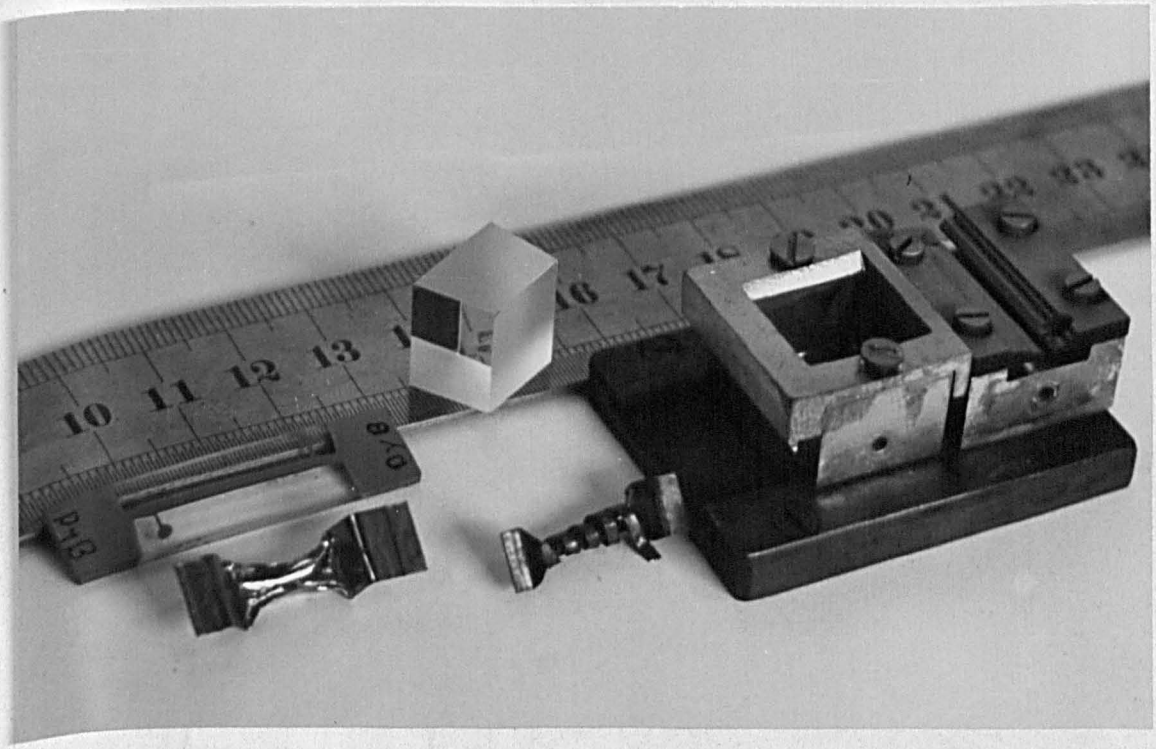

Photo. 1 Substrate Holder, Substrates, and Boats

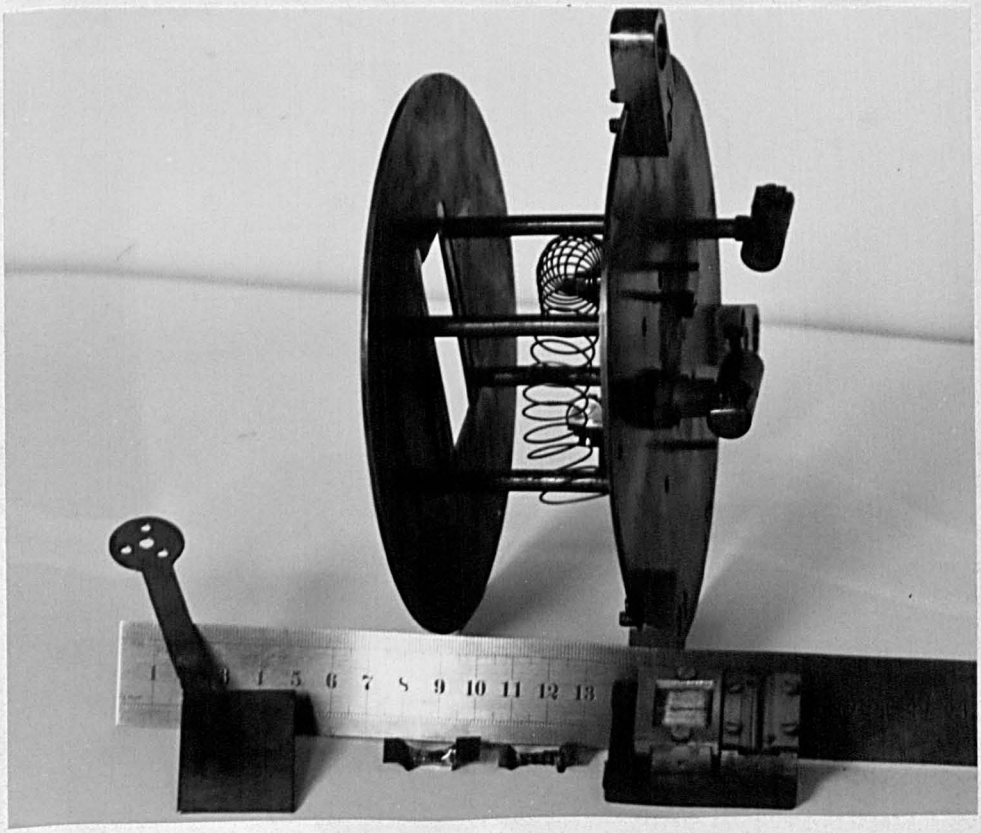

Photo. 2 Frame and Shutter

strates to atomic dimensions and, therefore, one may presume that the film is no rougher than the substrate. Since 10 Å roughness is typical of conventionally polished silica, a 5% error in conductivity is possible. However, this error is unlikely to modify structure as the error is a "well behaved" function of n and k.

It was hoped that roughness would explain the large difference with the present data Knyazev obtained for his measurements of bulk RE's. The change in σ using their data is in the right direction, but is too great in the uv and insufficient in the ir.

Roughness can also assist optical coupling to surface plasmons. Endriz and Spicer (1970) feel that such coupling will be minimal for metals with broad plasma resonances like transition elements. One can presume that the presently reported results were not significantly effected by surface roughness except to slightly lower the conductivity. Unfortunately purity is a more serious problem.

The metals used were claimed by the suppliers to be 99% plus pure. Other REM's < 0.1%, other base metals < 0.02%, and Ta and W impurity as follows:

Dy	trace	
Gd	present	R. T. Z.
Tb	present	(rare earth products, Johnson Mathey)
Yb	trace only	

Nd was obtained from Koch-Light who claimed it was 99.9% pure.

This means (except for Nd) that ~ 0.8% impurity is unaccounted for and is most likely gases and volatile solids as evidenced by the high pressure that results from heating the source materials. This is as much as 10^{-5} torr for the metals that sublimed and ~ 10^{-6} for the others.

Two samples of Dy were used one which had been worked (wire) and the other "sublimed xtal". As previously mentioned, efforts to reduce the pressure surge were only successful to the extent of reduction by one-half. The use of the crystal instead was much more significant; in one case the sudden rise in pressure did not occur. Though the crystal (with large surface area) appeared to be the poorer source, it was in fact much better. The deleterious effect of the other impurities is probably inverse to their concentration. This is because the most difficult impurities to remove are of course the other rem whose optical properties are very similar. The "other base metals" whose presence would be most damaging and are likely to be deposited with the rem are at most 0.02%.

The initial degassing pressure is $\sim 10^{-6}$ torr (10^{-5} Yb) and is reduced to an initial deposition pressure of $\sim 5\ 10^{-8}$ (10^{-6} Yb). That is more than an order of magnitude reduction of the remaining $\sim 0.8\%$. So that its effect on the optical constants is about that of the base metals. From the above, one can conclude that the films had an effective purity of $\leq 99.9\%$ including $\sim 0.1\%$ relatively harmless contaminant. Yb unfortunately is an exception; the best purity obtained is probably $\sim 99.5\%$.

The other source of contamination is the ambient gas during deposition which is mostly from the source metal and not residual, since a base pressure of $1\text{-}2\ 10^{-8}$ was always attained before heating the source. The effectiveness in avoiding this contaminant is most easily seen by comparing the respective rates of "deposition" of the ambient atmosphere and metal. Kinetic theory gives the particle collision rate per unit time and area, n as $n = P/(2\pi mkT)^{1/2}$, where the symbols are respectively, pressure, mass, Boltzmann's constant, and the temperature. For O_2 at 2.10^{-6} Torr, (the worst case), the rate is

$\sim 10^{15}$ molecules/cm^2 sec. Correspondingly, in the best case it is $\sim 2\ 10^{13}$. The deposition rate is found from the thickness and deposit time by assuming a constant rate over the $\sim$ 5-15 sec deposit time. This represents a minimum as it was probably higher at the beginning of deposition, a typical value is $5\ 10^{17}$. Therefore, the worst case represents 0.2% which is twice the expected contamination due to impure source material. However, a "sticking" probability of one has been assumed. The probability of O_2 on iron is known to be much lower ($5\ 10^{-3}$, Kroger, 1964). Of course, the metals studied were much more reactive. However, a value of 10^{-1} or lower is quite likely and is sufficient to make the principal source of impurity to be due to the boat and the source material. As can be seen from the foregoing, a very likely valid criterion for ambient atmospheric contamination is the division of the deposition rate by the pressure. This contaimination figure is given for the films discussed. That the films did indeed approximate the characteristics of bulk metal is indicated by the fact that the resistance ratio ($295^\circ K/78^\circ K$) of the four terminal test slide films was close to published bulk values.

Schüler (1966) verified that his Gd films did have nearly the same temperature dependence of their electrical resistivity as the bulk metal. This dependence was measured for two of the present films, Gd-7 and 5. Gd-7 had the poorest ratio (2.3X) of the annealed films and the change in slope at T_c was not sharp. Gd-5 test slide had the highest ratio at the time (3.24X). Its break was considerably sharper being unambiguously between 292.0 and $292.4^\circ K$. It was in fact a peak which Schüler did not obtain but is reported for the bulk metal. Furthermore, the break is $3^\circ K$ higher than his. Since impurities tend to lower ordering temperatures this

tends to confirm the correlation of the contamination and resistance ratio criteria. (Schuler's film had a ratio of 3.18X). Another indication of whether the films will have optical properties characteristic of bulk metal is given by comparing their resistivity to that given for the bulk metal.

The resistivity of a number of the co-deposited test slides was found by measuring the dimensions of the film strip. Unfortunately the thickness measurement (by multiple beam interferometry) is subject to large error, mainly because the thickness along the strip varied by as much as 75%. This was because the source to substrate distance was as short as 3 cm. Therefore, for the following data an error of ~10% may be assumed. The Gd films were found to have a Rt ρ range of from 150 to 180 $\mu\Omega$ cm for 13 films. Their resistance ratios were well correlated and had a range of 1.7 to 4.2X; the corresponding bulk values are 130 $\mu\Omega$ and 4.3X. The thickness of only one Yb slide was found giving a ρ of the bulk value. All of the annealed films had ratios significantly greater than the bulk value. The resistivities and resistance ratios for the Dy and Tb films are tabulated below.

Film	Dy-5		Dy-X	Bulk Dy	Tb-1	Tb-2 (unannealed)		Bulk Tb
ρ	100	cm	130	93	121	154	(167)	115
ratio	3.1X		2.05	3.32	3.25	2.53	(1.68)	3.84

None of the Nd films were measured for thickness. However, the ratios except for the unannealed films were very close or exceeded the bulk value (2.17X). It is felt that the preceding is good evidence that the films do characterize the bulk metal at least for the electrical resistance.

It was found difficult to relate the resistance and deposition criteria to the optical "quality" of the films. This is because the optical

interaction with the metal is limited to a surface layer of only a few hundred Å's thickness. Therefore, the surface may be optically "ruined" without effect upon the dc electrical characteristics. If the measured surface had been the first, there would be less problem as atmospheric contamination reduces the conductivity of absorption peaks (Liljenvall et al., 1970; Pells and Shiga, 1969).

In the present case, reaction with the substrate instead of with the atmosphere is the principal source of the lack of reproducibility for Nd, probably Yb, and possibly dysprosium. The effect of substrate-metal reaction is quite striking in Nd and is discussed in Chapter 4. Yb is more difficult to evaluate as all three films were measured long after preparation. Their ratios were nearly the same. Substrate reaction may have been the cause of the contradictory effect of annealing upon Dy and to a lesser extent Tb. Annealing always increased the degree of change in σ due to magnetic order, and also the ratio. But the optical conductivity was reduced. The necessity of annealing to reveal the effect of magnetic order in Dy is quite striking. This can be seen in Fig. 3.2 where a cooled unannealed film Dy-X only very slightly shows the effect of magnetic order while it is quite obvious in Dy-5 a poor "quality" (resistance ratio) annealed film. Gd was normal in that annealing, ratio, optical conductivity and conductivity change with magnetic order were all positively correlated. Gd of course reacts minimally with silica as shown in Fig. 3.1.

Preparation of a film typically was done as follows: The source material was washed with electronic grade acetone and placed in a previously degassed boat (new if a new metal is being used). The substrates were cleaned in chromic acid and rinsed well with acetone. To prevent con-

densation of water with atmospheric dust, the substrates are allowed to dry in a saturated atmosphere of acetone vapor. This is provided by placing the prism immediately after rinsing on acetone soaked kim wipes under an inverted beaker. This method invariably left a perfect surface as seen visually. Until this method was adopted, imperfections were often seen on the prism surfaces. AThen the substrates were mounted along with two resistance monitors. The chamber was roughed by opening in succession the two sorption pumps. The resistance monitors were constructed of slides with W wire imbedded in the ends. Fired PtCl was used to make electrical connection with the wire and the to be deposited film. The slides were placed such that one was coated with the shutter closed and open and the other only with the shutter open. When the vac-ion pump was started, the substrate heater was turned on and gradually increased in power as allowed by the pumping rate of the pump. Usually full power ($\sim$ 240W))was attained by 10^{-5} torr and maintained for at least 15 hours. At that time the heater was shut off and by the time the interior had cooled to $\sim 50^{\circ}C$ the pressure was $\sim 10^{-8}$ torr. The metal to be deposited was degassed by evaporating $\sim$ 1/3 of the charge ($\sim$ 2 gm). This was done in a few seconds for those that melted and for Yb and Dy more than an hour. After a short cooling period, the boat was again heated and evaporation commenced.

When the pressure had dropped to the low 10^{-8} range, or if not possible, when approximately another 1/3 of the charge had been evaporated, the shutter was opened for $\sim$ 10 sec. The boat was then cleaned for reuse of the same metal. This was done by applying significantly more power for a time after which no further evaporation occurred, as shown by the monitor slides. The

pressure was continuously monitored during degassing of the source and deposition by a pen recorder connected to the log. current function generator of the pump power supply. Its time constant was shorter than that of the pump pressure meter. Since the surge on opening the shutter had a width of ~ 0.5 sec, it is assumed its height was not electronically degraded. If the film was to be annealed, it was immediately done by applying full power to the heater until the temperature was near 250°C. (The pressure was always significantly lower than the initial pressure during deposition.) It was usually then shut off so that the maximum temperature was ~ 300°C. If it was desired to maintain the temperature for some time at 300°C (15 minutes), the power was maintained at an appropriate value. When cool, the system was opened and the resistance ratio of the 4 terminal film was determined using a 10 ma current and a potentiometer or digital volt meter. At no time was non ohmic behavior observed. It was found quite satisfactory to immerse the slide directly in the ℓN_2. Connections were made with In solder then the slide was over coated with silver.

The films were measured by an ellipsometer designed and constructed previously under the direction of Dr. Hodgson. It was used with only one modification to be discussed later. A short description of the instrument will be given followed by an examination of details which are important with respect to error.

An overall view of the ellipsometer is shown in Photograph 3. The tungsten filament light source is the second element from the left on the optical bench. It is used for the ir and visible. For the uv, a deuterium discharge lamp was used. The element to the extreme left is

the

the first mirror and is ~ 12 cm from the lamp and has sides of length 2.5 cm. Just to the right are the third and second mirrors in order of light path. The analyser follows and then the chopper driven by a synchronous motor. The pencil is chopped at a frequency of 800 Hz. The reference lamp and condensing lense can also be seen. Behind the chopper blades is the reference generator, an OAP12 photodiode. Just before the vacuum tank is the entrance aperture and just after the exit aperture. The polarizer, two further mirrors and the prism [illegible] spectrometer complete the optical apparatus. The power supplies for the tungsten and D_2 lamps are on the extreme left and rear. The insulated liquid nitrogen reservoir is next to the vacuum tank. Not visible on the right is the H_2 purifier which supplies a thermally conductive dry atmosphere to the vacuum tank when used for low temperature measurements. The PbS (Mullard, 61 s v) cell is mounted on the spectrometer. Its exciter (15 v - 2.2 megΩ) is underneath the spectrometer. A photo cell (Mullard, 150 uv) is substituted below ~ 0.5 μm. The spectrometer shown contains a 30° silica prism. When more light is desired, a similar one using a 15° prism is substituted.

Photograph 4 illustrates the method of rotating the prism and the entrance slit. Since high resolution was not desired, the slits are rather crude and were adjusted simply by turning a thumb screw from a 1/4 to 3/4 of a turn from the closed position. The optical arrangement was symmetrical using two concave mirrors and a double pass through the prism.

As previously discussed, in order to avoid using a diffusion screen, a tungsten strip lamp is used. When new they emit unpolarized light normal to the surface, with age polarization may amount to a few percent (Bennett

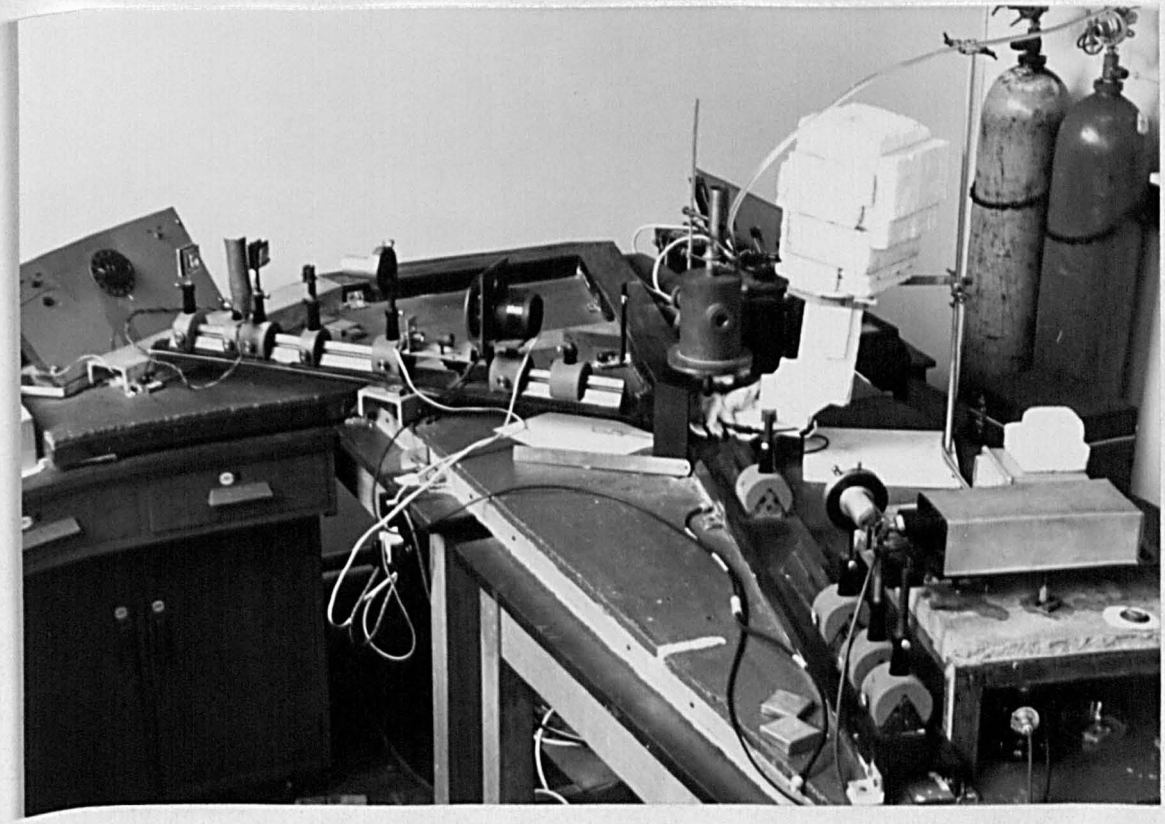

Photo. 3 Overall View of Ellipsometer

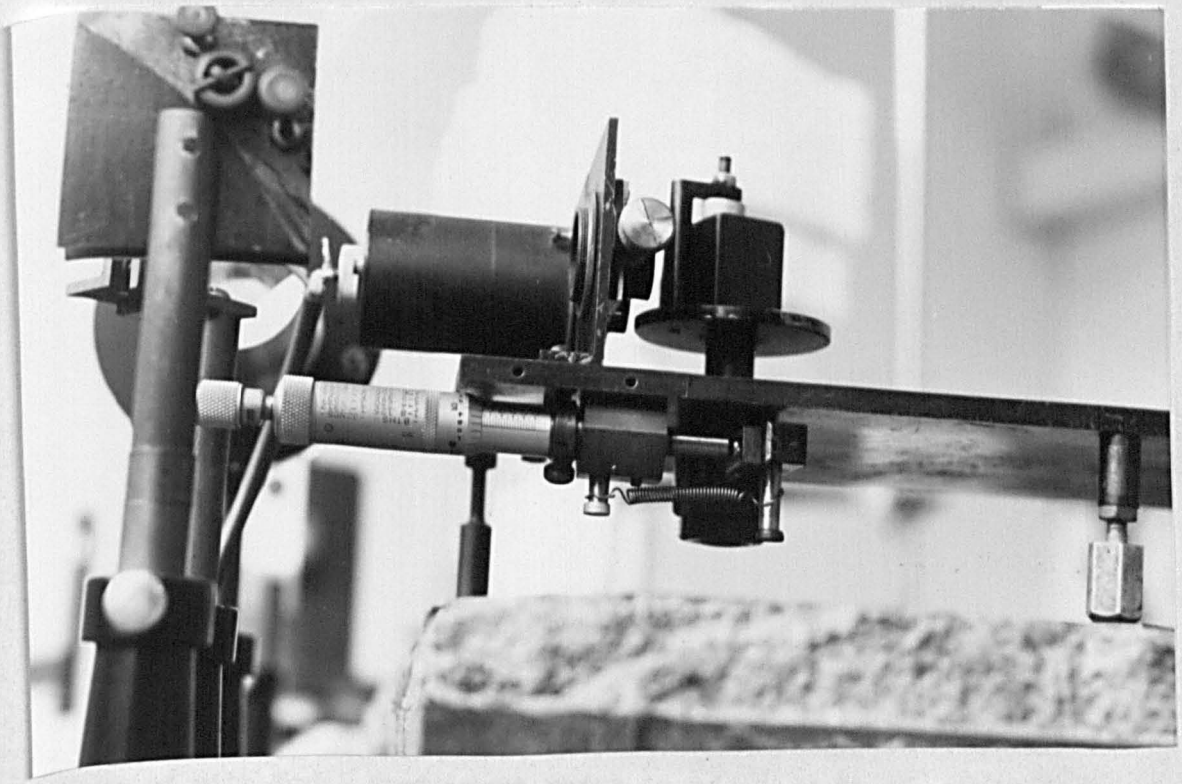

Photo. 4 Prism Spectrometer

and Bennett, 1967). The first mirror limits the emitted light to a cone with an 1/2 apex angle of 6° so that polarization from non-normally emitted light is not a problem. The tungsten light source was supplied from a constant voltage transformer and consequently drift from this source was not noticed $\leq 0.1\%$. The same is true of the D_2 lamp which was stabilized by Balast Lamps. The polarizers were Rochon (quartz) prisms. Unlike the usually used glan-Thompson, the beam is not deviated by rotation; especially important if the beam is not uniformally intense, both because of the restriction by the aperture and possible non-uniformity in the film.

The degree of uniformity of a Dy film was found by inverting a prism after measurement. The differences found were much less than the changes between measurement points.

Some difficulty was encountered in cooling the films to liquid nitrogen temperature. Though the tc shown in Photograph 6 indicates liquid N_2 temperature when the pressure in the tank was low ($\sim 10^{-3}$ torr), it became obvious when measuring Dy that the actual film temperature was much higher. One solution was to measure with a high H_2 pressure, at least 0.2 torr, in which the minimum possible temperature was $\sim 86^{\circ}K$. However, at this pressure, the tank was cooled to such an extent that water sometimes condensed on the windows. In an effort to reduce the pressure and the temperature or at least maintain it, a cylindrical heat shield was made to supplement the existing one (shown in photograph 5). Exit and entrance holes of the minimum possible size were cut. In addition, since it was made of brass, it was copper plated to increase its reflectivity. The inside was painted with Kodak instrument paint in addition to the appropriate surfaces

Photo. 5 Prism in Place on Sample Table, (note low temperature heat shields).

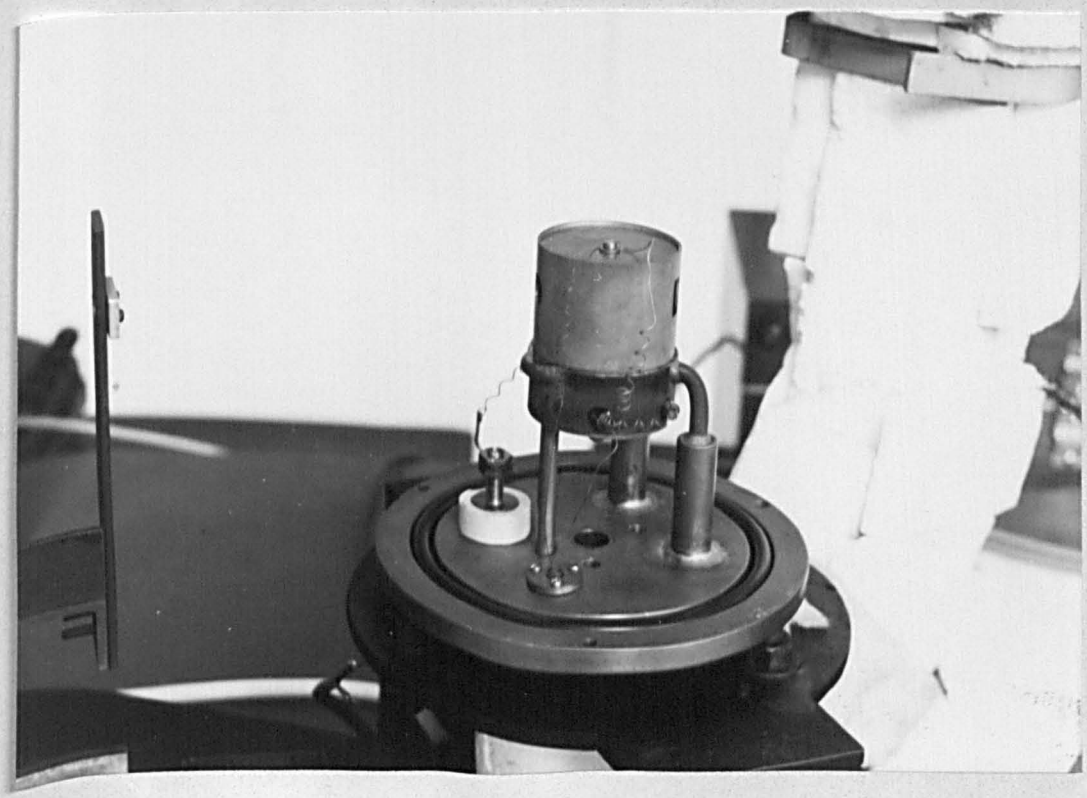

Photo. 6 Heat Shields and Thermocouple in Place for Low Temperature Measurement.

of the existing shield. Lastly, Heat sink-prism contact was improved by using a drop of diffusion pump oil. All of these measures made it possible to lower the pressure to $\sim 10^{-2}$ torr before the temperature of the prism rose as evident by a change in the angle for maximum intensity using a Dy film. It was also noticed that the radiation from the tungsten source warmed the film when low pressure was used with the radiation shield.

To illustrate the effectiveness of these changes, Fig. 3.2 shows that rt σ of Dy X and the ℓn_2 measurements made before and after the discovery of the thermal isolation of the film. Dr. Hodgson's measurement at high pressure done (without the new shield and contacting fluid) to show the thermal isolation of the film is also included. The obvious improvement over even Dr. Hodgson's data taken at high pressure is to be expected as the new shield reduced the effective aperture seen by the film by a factor of 10X. Photograph 6 shows the shields in place and the tc clamped in place.

The spectrometers were calibrated using a Hg discharge lamp. More than 10 lines were used with each, fitted to the equation:

$$D = (A - \text{Index})B^{-1} + C$$

where D is the drum reading (micrometer), A, B, and C are the fitting constants and Index is the index of silica found from an equation given by Malitson,(1965). This is the same equation used in Eq. 12, Chapter 1. Since the 30° spectrometer was used over such a large range two B's were used. The change being when D became equal to C. The maximum deviation found in fitting to the Eq. for both the spectrometers was approximately $\pm$ 30 Å.

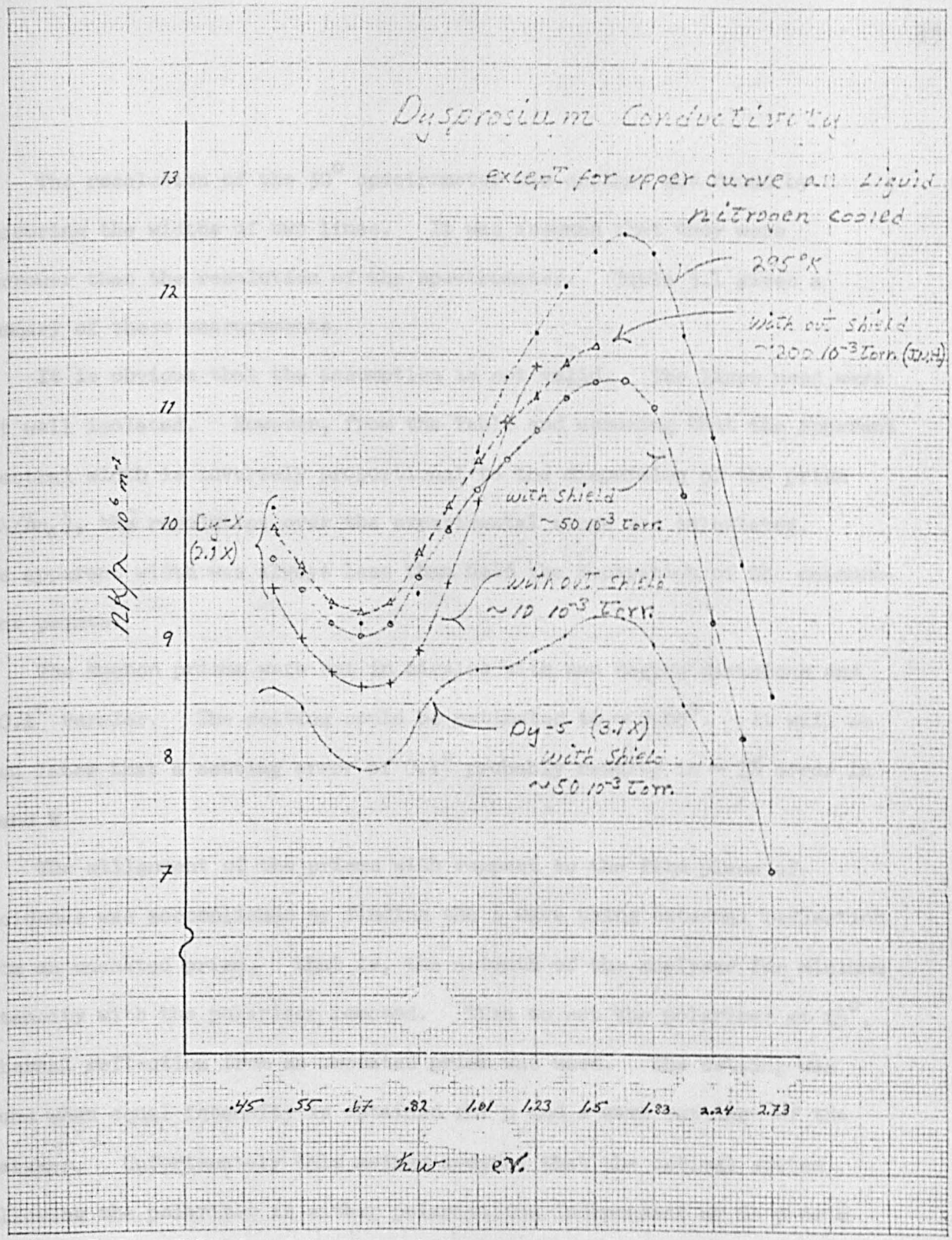

Fig. 3.2 Effect of Heat Shield

The resolution of the 30° spectrometer was defined and found by measuring the widths of two lines. It was assumed that they were narrower than the resolution of the spectrometer. Table 3.1 gives a summary of these measurements.

It is obvious that the assumption is not valid. The lines used were not well isolated. However, from the Table and assuming that the apparent spectral width is inversely proportional to the dispersion of the prism $(\Delta\lambda/\Delta n_0)$, the resolution over the experimental range was calculated. The apparent width was always less than half the separation of the measurement points.

The Rochon prisms were set in circles with one degree divisions and a 0.1° vernier. The setting could be estimated to $\sim 0.05^{\circ}$. It will be seen later that a setting error of 0.1° probably results in $\sim 1\%$ error in n and k.

The allignment of the prisms with respect to the film plane of incidence was accomplished by finding the ρ wave using external reflection from an uncoated prism, that is, the azimuth of the analyser for minimum intensity with the polarizer removed. Then to set the polarizer at 45°, internal reflection from an uncoated prism was used. The setting was found when equal intensity is obtained for p and s wave settings of the analyser. Unfortunately this method assumes that the optical system following the polarizer is either polarization independent or is p or s polarized. This was not realized at the time and, therefore, an unknown systematic error may have been introduced.

The electronics consisted of a high gain low noise amplifier and a phase sensitive detector. Originally these were non commercial and the volt meter

TABLE 3.1

Slit Width	Δλ	ΔeV	ΔeV/eV(%)
		1.71 μm (0.725 eV)	
1/8	220 Å	.009 eV	1.3%
1/4	290	.012	1.7
3/8	420	.018	2.5
1/2	850	.037	5
		.577 μm (2.15 eV)	
1/4	125 Å	.047 eV	2.2%
1/2	200	.075	3.5

was a portable galvanometer. After Gd was measured they were replaced by Brookdeal models LA 350 and PM 322 and a Solartron digital volt meter, LM 1620. The drift and non linearity claimed for this system, excluding the detector, are < 0.2% FSD, which is less than the sensitivity to the analyser setting or the noise. An overall check of the linearity of the system and the allignment was done by testing Malus' law. The results are tabulated below:

Polarizer orientation	Error from Malus' Law (%) with respect to 0°	60°	45°
0	-	1.5	1.0
30	3	.7	.2
45	.5	.7	-
60	1.0	.-	.5
75	2.0	1.5	2.0

The source of this error was not sought but it may be due to either polarization of the light source or non linearity in the detector. Below 3eV detector non linearity is not serious as the intensity variation encountered is < 5:1. However, in the uv intensity ratios as high as 50:1 are encountered.

The directly measured quantities were the inclination of the ellipse (τ) and the intensity ratios of the p and s waves and the ellipse axes. The angles ψ and χ are defined as the tangents of the square root of these ratios. The change in intensity with analyser azimuth is small at the minima and maxima. Therefore, τ (φ max) was found by averaging the angles at which the intensities are equal for angles displaced ~ 40° from φ max. Repeating this procedure indicated that the random error was rarely more

than $\pm$ 0.05° in the region 0.5-3 eV. As a direct check on the effect of error in γ, a measurement series was made with γ displaced 0.1° from the measured value. n and k were changed by $\sim$ 0.02 (< 1%) and σ changed 0.04 (< 1/2 %). Unfortunately, since the effect is opposite in n and k, n^2-k^2 suffers an error of 0.24 or $\sim$ 3%.

The error in the intensity ratios was highly variable being subject to the signal to noise. This depended on the signal which was a function of the reflectivity of the film, and the available light. In general from 0.5 to 3 eV. the maximum signal was large so that the signal to noise was > 1,000:1. At the reflectivity minimum (minor axis) at 3 eV it could be as low as 150:1. At higher energies the ellipticity became extreme and the available light fell off. The table below gives the percentage noise/signal for data taken from a Dy-B, one of the worst cases.

$\hbar\omega$ (eV)	I_{max} (n/s %)	I_{min} (n/s %)	γ (°)
3.3 eV	.07%	.6%	-30.6°
3.7	.07	1.0	-32.3
4.0	.1	2.0	-33.5
4.5	.2	4.0	-34.2
5	.3	15.0	-34.7

The table illustrates the effect of using an unsuitable prism angle. At the principle angle γ is zero and the axial ratio is maximum. As the absolute value of γ increases η diminishes. In general if $|\gamma| > 30°$, the ratio of the axes is > 10. For example from two ytterbium films:

$\hbar\omega$	$\tan^2\eta$	γ	$\tan^2\eta$	γ
.5 eV.	.06	39	.38	-17°
3.7 eV.	.44	-18°	.03	-42°

It is difficult to relate the error in the intensity ratios and γ to the error in optical constants. However, Conn and Eaton (1954) used the same method of determining Δ and ψ as in the present work. They calculated $\frac{\Delta K}{K}$ and $\frac{\Delta S}{S}$ as a function of ψ at the principal angle of incidence. Unfortunately, K and S^2 are not easily related to the conductivity which is the most useful optical constant, but are equal to k/n and $n^2 + k^2$. However, their calculations indicate the error expected. $\Delta K/K$[1] has a value < 10 for $15^\circ < \psi < 40^\circ$ or intensity ratios between $\sim .07$ to 0.7. While $\Delta S/S$[1] is < 10 from 0 to 30° rising steeply thereafter. In the worst case (Yb-2) ψ is $> 35^\circ$ over half the experimental range with a maximum at 40°. $\Delta S/S$ is ~ 20 at 35° and 40 at 40°. These values must be multiplied by the noise to signal and divided by the reflectivity. The reflectivity (at normal incidence) was always greater than 7%. Therefore, it can be expected to be usually above 0.5. This means that below 3 eV the values are $< 10\%$ and above 3 eV. The extreme value is over 100%. It is not clear what effect measurement far from the principal angle has on Conn and Eaton's result.

These values may be compared to the experimental scatter found in the conductivity data. The table below is from data from Dy-B which is typical.

$\hbar\omega$	1 eV	2 eV	3 eV	5 eV
$\Delta n_K/n_K$	1%	2%	4%	20%

Duplicate points are given in the graphs specifically to indicate the probable error and the lack of consistency due to ageing, use of different

[1] For computational purposes the noise to signal and intensity reflectivity has been set equal to 1.

spectrometers, and lack of temperature control. From this it can be seen that improvement in the quality of the films is more pressing than improvement in the ellipsometer.

CHAPTER 4

EXPERIMENTAL RESULTS

Gadolinium

The optical constants of three of the seven heavy rare earth metals were found. Gadolinium was the first metal investigated as extensive work had already been done by C. Schüler (1966). He used the transmission reflection method to find k and n. Since then at least three other groups have measured one or more of the HREM's. They are Knyazev(70, 71, 71a); Petrakian(72); and Erskine(73). The conductivities[1] for Gd found by these groups and this work are shown in Figure 4.1. There is considerable disagreement among them, which is probably due to radically different preparation conditions. The exception is Erskine's moke[2] data, (No.7) which must be different and is discussed later. As explained in Chapter 3 the contamination criterion (deposition rate/ambient pressure) will be used to indicate the probable "quality" of films. Figure 4.2 includes Erskine's "normal" conductivity which compares favorably with the presently obtained conductivity. The criterion for his films was between 0.2 and 1.0 m $(s\ torr)^{-1}$ and were measured in situ ellipsometrically. Measurement was done under a pressure of less than $1\ 10^{-8}$ torr. The present results shown were taken from films Gd-12 and -2 with criteria respectively of 2 and 0.5 m $(s\ torr)^{-1}$ or better.

---

[1] The general theory discussed in Chapter 2 will be used to discuss the results given in this chapter in Chapter 5. It will consist largely of the analysis of the conductivity in the light of band calculations. Therefore, in this chapter the present results will be presented in the form of conductivities.

[2] Magneto-optical Kerr effect, (p.82).

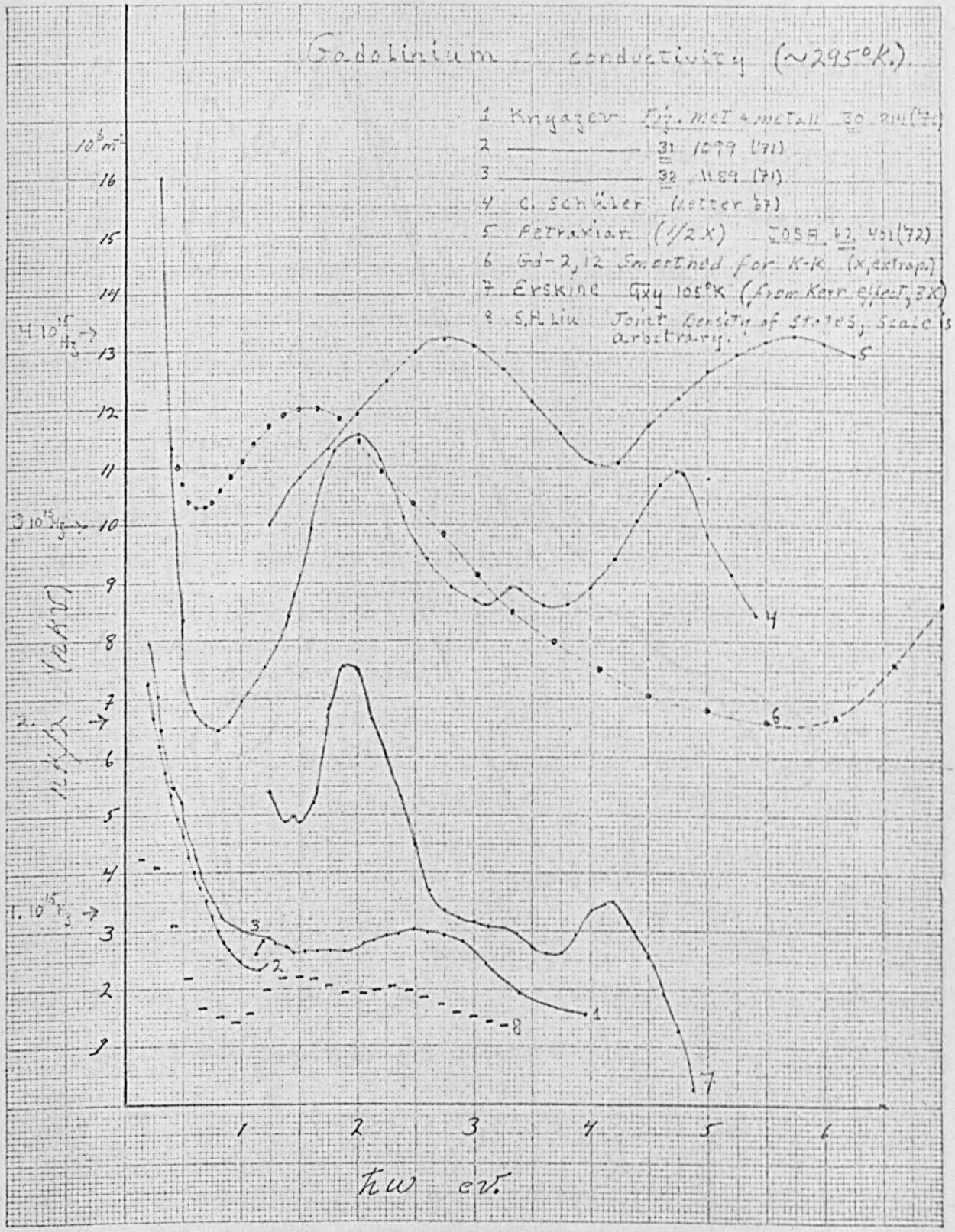

Fig. 4.1 Gadolinium - Present and Previous Work Comparred

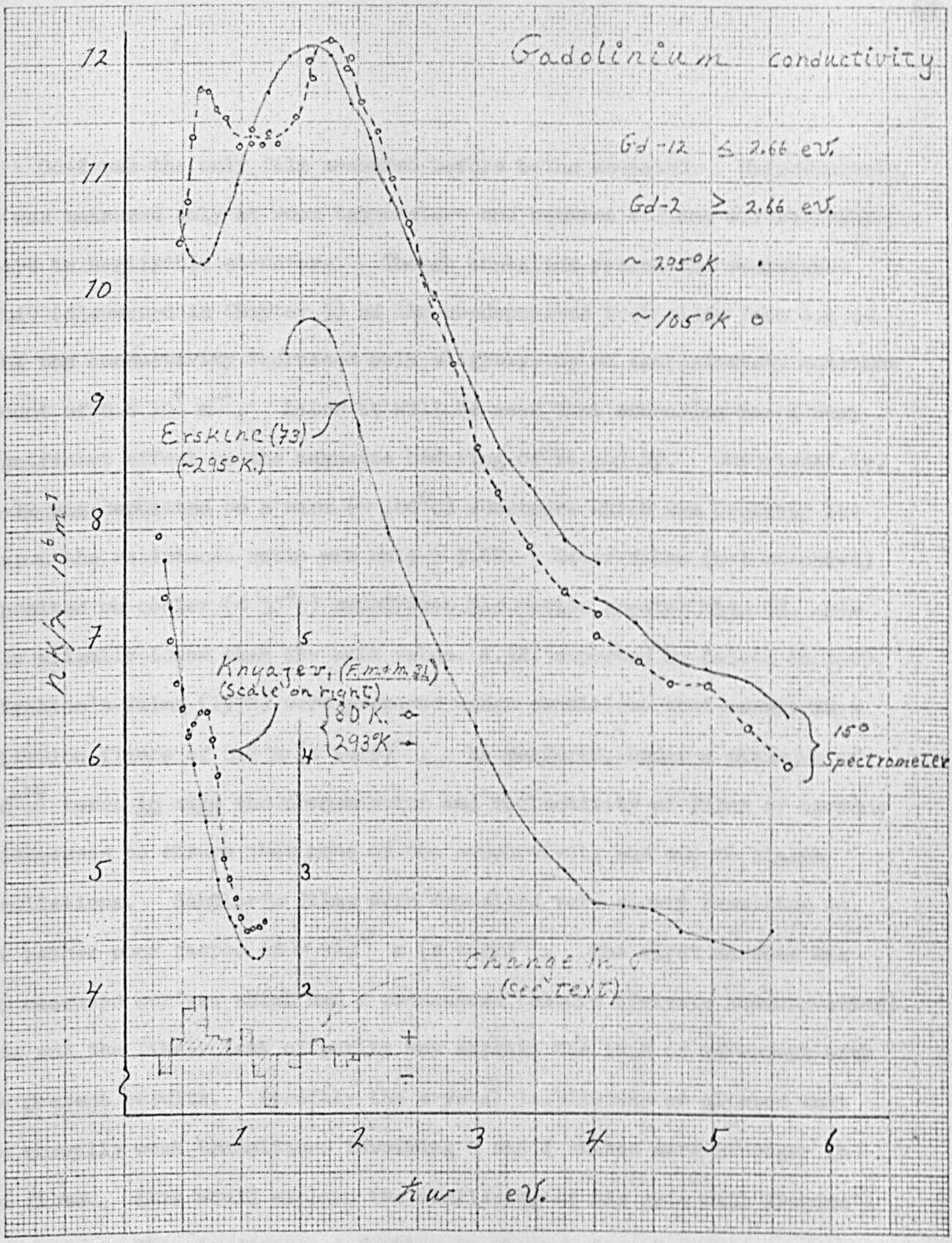

Fig. 4.2 Gadolinium - Effect of Magnetic Order

Gd-2 was the only film measured before being annealed. Unfortunately, it was measured only at room temperature and between 2.1 and 4.2 eV. where there is negligible structure. Though annealing raised the resistance ratio (discussed in Chapter 3) of the co-deposited test slide from 1.6 to 4.0X the conductivity increased only slightly, by an approximately constant amount of $0.6\ 10^{6}\ m^{-1}$. Later it will be seen that annealing has a very significant effect on the magnetic ordering of tb and Dy. Unfortunately, Gd-12 was deposited on a warm ($\sim 100^{\circ}C$) substrate which was probably the reason the resistance ratio was only $\sim$ 3.6X. Later films (not measured) deposited on cooler ($< 30^{\circ}C$) substrates had ratios greater than 4X, some only slightly lower than the bulk value, 4.3X, reported by Colvin in 1960. Petrakian's films (1972) were prepared under conditions that result in a criterion figure of 0.2 m $(s\ torr)^{-1}$. He measured, under a pressure of $5 10^{-10}$ torr, <u>in</u> <u>situ</u> the transmission and reflectivity of films of various thicknesses to ensure that none of the conductivity was due to plasma oscillations. Schüler's films were deposited very slowly resulting in the rather poor factor of $\sim 2 10^{-2}$ m $(s\ torr)^{-1}$. The first surface was the measured surface which had a pronounced texture (Private communication). This and the likely lack of purity may explain the lack of agreement with the present results. Possibly the crystal lattice was so altered that the normally weak transitions involving d and f states were stronger in his films. This would explain the similarity of his data with Erskine's moKe data. This is discussed further in Chapter 5. Knyazev's samples were bulk metal preserved after mechanical polishing in a N_2 atmosphere, and measured a few hours after preparation. The variation of n and k was only 5% in two days, while 25 - 40% changes occurred when

measurements were done in air. As discussed in the previous chapter an attempt was made to explain his significantly lower conductivity as being due to the high surface roughness expected from mechanical polishing. This largely failed indicating that efforts to protect the surface were not completely successful. It is quite likely that an initial oxide film forms immediately which protects the surface from further contaimination, but leaving the surface already no longer characteristic of the metal. Another possibility is that lattice defects caused by the polishing is significant. Mechanically ground and polished surfaces suffer lattice distortion to a depth of 2 or 3 times the diameter of the abrasive used. (Bennett and Bennett, 1967) So that even 1/4 μm diamond powder used as a final polish will leave a distorted surface deeper than the optical penetration depth. Whether this effect is important or not could be easily determined by annealing.

Terbium

Two films of Tb were prepared. In both cases the maximum pressure during the deposition was less than $4\ 10^{-8}$ resulting in the excellent contamination figures of 5 and 2.5 for Tb-1 and Tb-2 respectively.

Tb-2 was measured before and after annealing. The effect of annealing is quite striking and may be seen in Figure 4.3. Tb-2's resistence ratio was raised from 1.7 X to 2.5 X by annealing. Tb-1's ratio was 3.3 X which is ~13% lower than the bulk value of 3.8 reported by Colvin (1960). Petrakian also measured Tb, but his results are not reproduced because of their great similarity to his Gd results.

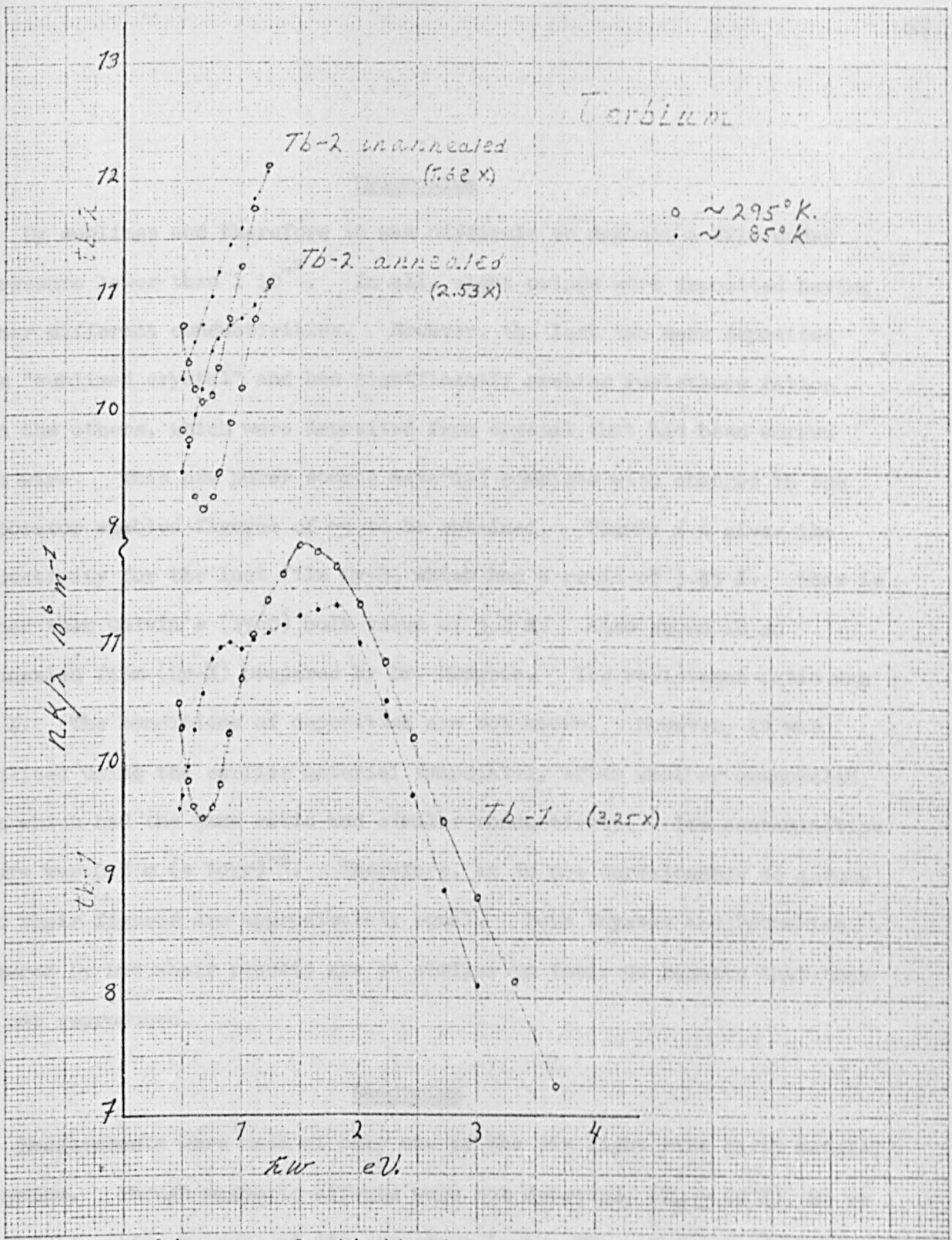

Fig. 4.3 Terbium Conductivity in Para- and Ferro-magnetic States

Dysprosium

Dy sublimes and therefore it was difficult to deposit a film under a pressure lower than 1 10^{-7}. In all, eight prisms were deposited having rather different conductivities. However, the last two were deposited from "sublimed crystal" and had significantly greater resistance ratios than the others, which were deposited from crystal that had been worked into wire. This new purer source material combined with changes in the evaporator enabled figures of ~3 to be obtained. Figure 4.4 gives the conductivity for the last film Dy-B, which had a ratio of 3.45 X. This is higher than Colvin's (1960) bulk value of 3.3 X. Also shown is an unannealed film (Dy-X) prepared by Dr. Hodgson. Its resistance ratio was 2.0 X. The conditions of deposition are not known. However, it was deposited using the earlier material immediately after another unannealed film which had the same ratio and similar conductivity. Its contamination figure was 0.3 m (s torr)$^{-\frac{1}{2}}$. Therefore, it is not unreasonable to assume that their figures are approximately equal. Both Knyazev and Petrakian measured Dy but their results are so similar to their Gd results that they are not reproduced.

Neodymium

Measurements were made of only one of the six light rare earth metals, neodymium. Though magnetic effects were not detected, ($T_N \simeq 20^{\circ}K$), Nd is quite interesting because of its structure in the IR. This structure consists of two (possibly three), weak peaks superimposed on a strong absorption peak. All the other lanthanides have only a simple strong featureless peak in the IR.[1] This structure is so weak (~2% in σ) that

---

[1] It is possible that all of them have inter band absorption below the limit of the present experimental range. Knyazev found one in Gd (Fig.4.1 No.3) and Yb also, as indicated by the Drude extrapolation (Chapter 5).

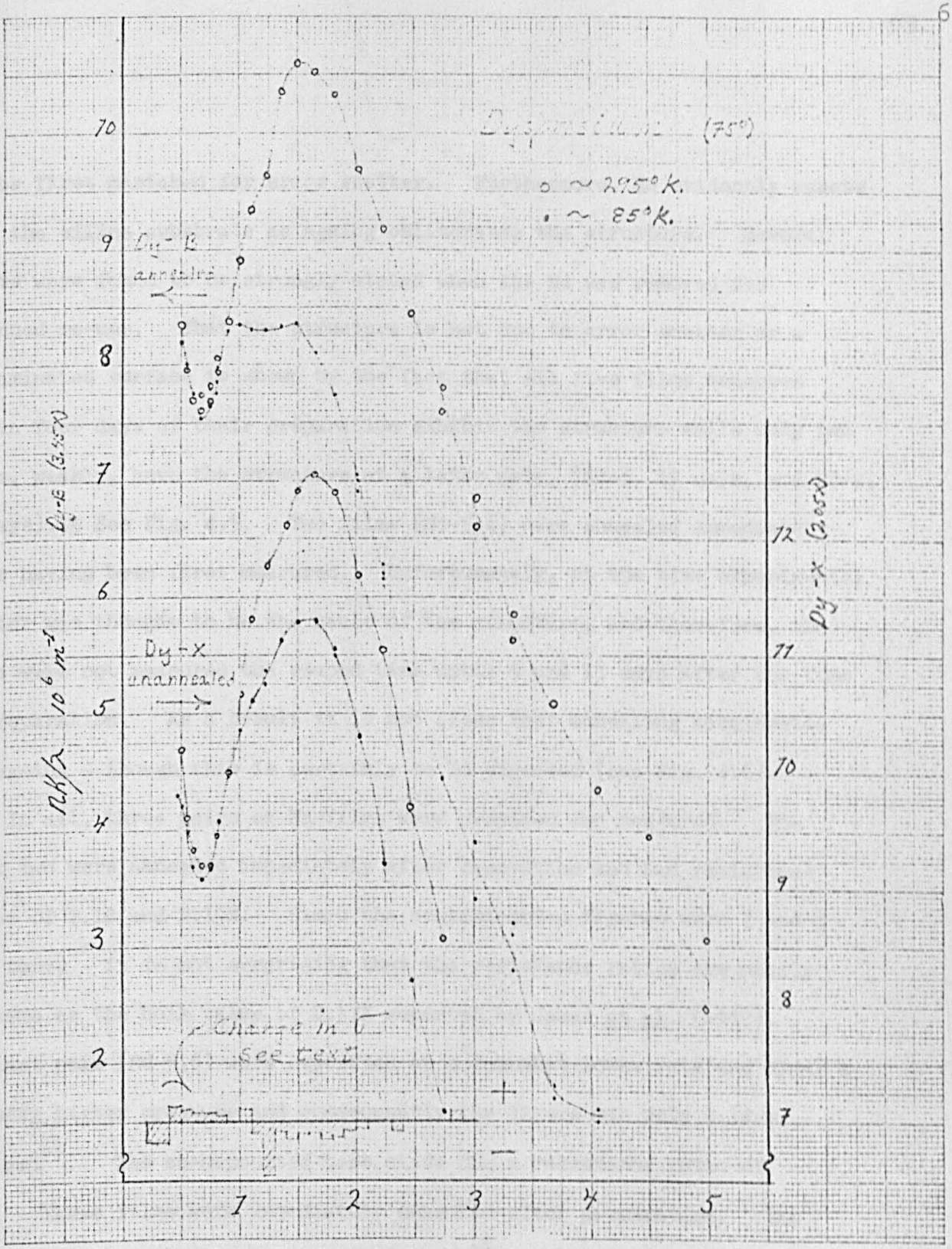

Fig. 4.4 Dysprosium Conductivity-Para- and Ferro-magnetic States

it was first mistaken for error scatter. Furthermore, Nd evidently reacts with the silica substrate as ageing obliterates the structure. Several prisms were found to be strongly etched when the Nd was removed for intended re-use. That the structure is not due to error scatter or a contaminated surface is shown by the fact that all five films measured within four days of their preparation exhibit the structure while only two films, weakly, have the structure at a later date, (Nd-5, 15 days, and Nd-2, 22 days). See Fig. 4.5. Two films (Nd-5,6) were annealed immediately after having been first measured. Unfortunately, at the time experimental scatter was thought to be the cause of the structure, and therefore, the films were not measured the second time until 5 and 15 days after the time of preparation. As a result it is not clear that annealing accelerates the ageing - though this is certainly to be expected (see Fig. 4.6).

In all, three pairs of Nd films were prepared and measured. The first two were annealed immediately after deposition and had resistance ratios of 2.18 and 2.19X. Since the contamination figures were 7 and 3 m $(s\ torr)^{-1}$ it is not surprising that the resistance ratios are nearly the same as the bulk value of 2.17X reported by James et al. (1952). The last pair (Nd-5,6) were deposited at a somewhat lower rate and under a slightly higher pressure and consequently the figure was only 0.14 m $(s\ torr)^{-1}$. The co-deposited test slide had a resistance ratio of 1.75. These films were immediately measured after preparation. The measurements were done under vacuum ($\sim 5\ 10^{-3}$ torr) and within a few hours were returned to the high vacuum system and annealed. After annealing the ratio increased to 1.95. It is evident that ageing is the principal factor in the variation of Nd's conductivity. Atmospheric

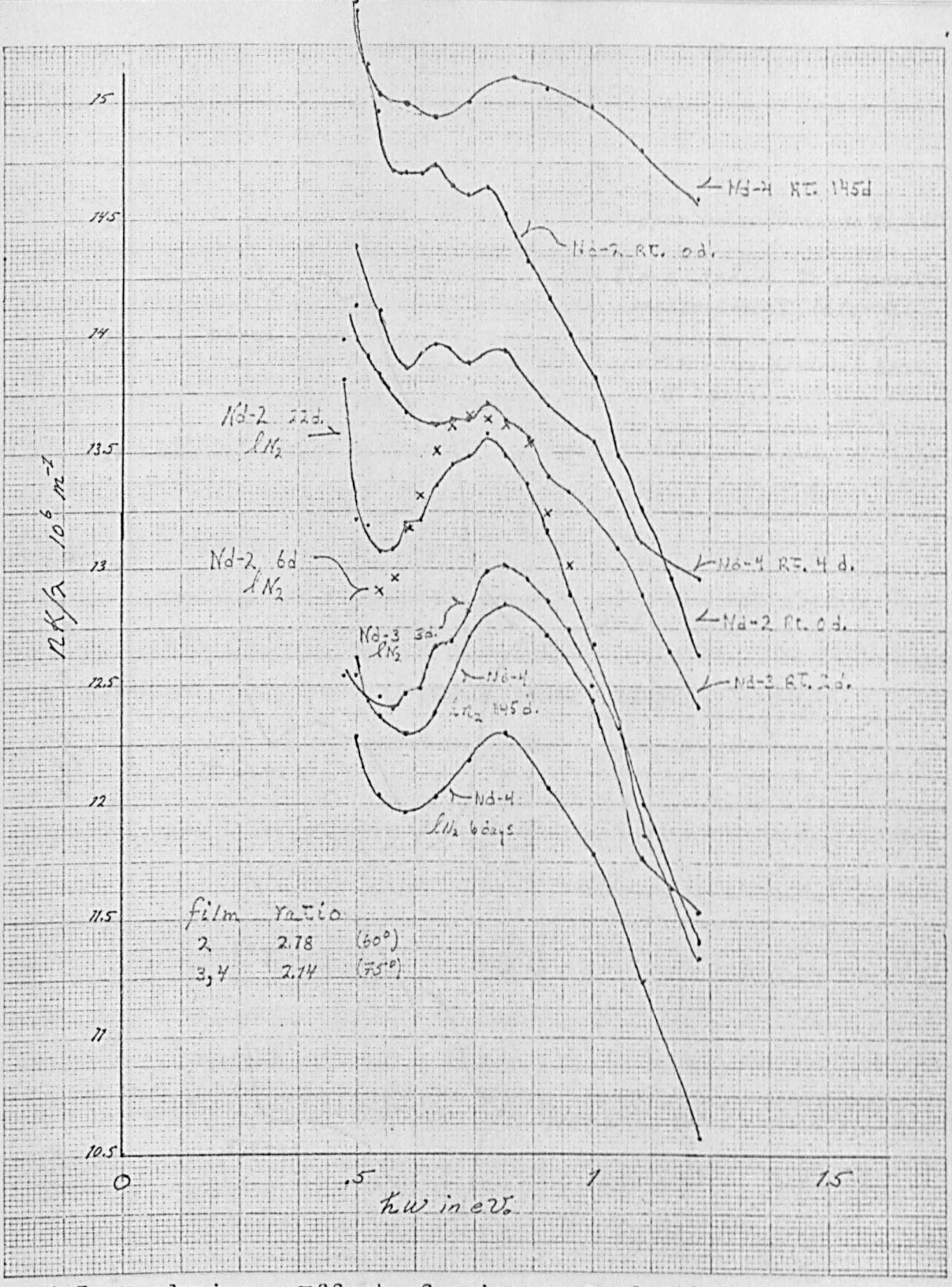

Fig. 4.5 Neodymium - Effect of aging on Conductivity

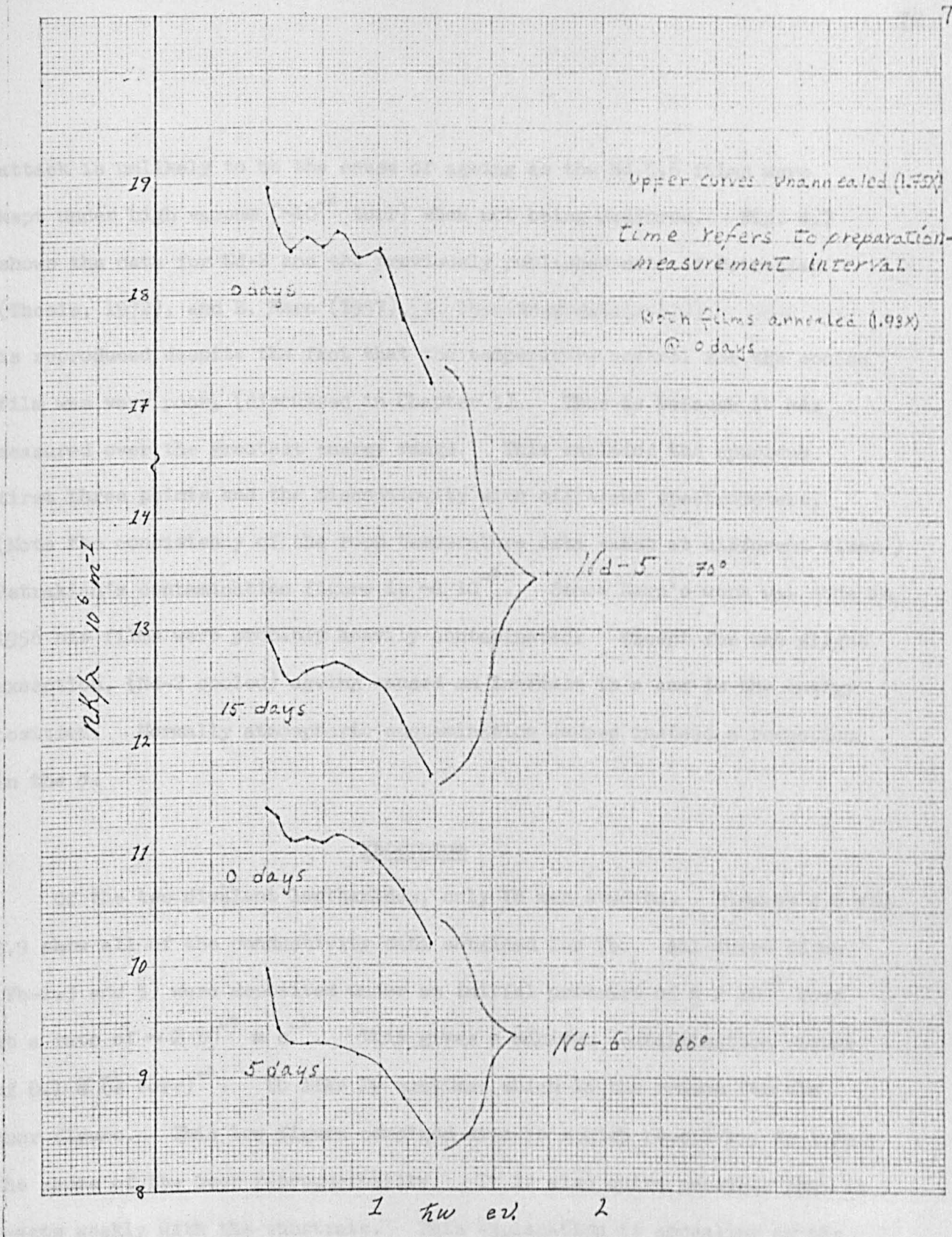

Fig. 4.6 Neodymium - Effect of Annealing and Aging on Conductivity

attack is unlikely to be the cause of ageing as the Nd-5,6 films were kept under high vacuum ($\sim 10^{-8}$ torr) when not being measured. Fig. 4.7 shows the data for Nd-2 and the previously published data of Petrakian (Thesis, 1972), and E. Kern (1957).[Z. Physi Nd-2 data (1957)]. Nd-[illegible] is reproduced despite the fact that the temperature control for the cooled film was very poor, (discussed in Chapter 3). This is because it was measured over the greatest energy range. This explains the spurious first three points and the discontinuity with different spectrometers. (Note the consistency of the room temperature data taken at different times) Petrakian's contamination figure is $\sim 2\ 10^{-2}$. Since Kern's work was done in 1956 his films were probably heavily contaminated. Except for one slight exception, (Nd-2 cooled) ageing caused an increase in σ and in the energy position. Normally atmospheric contamination causes instead a reduction in the σ.

Ytterbium

Of the two divalent lanthanides, only Yb was studied. Figures 4.8 and 4.9 show all of the conductivity data obtained for Yb. All three films (Yb-2,3 and 5) were deposited under an initial pressure of $\leq 2\ 10^{-6}$ torr at a rate of $\sim 2\ 10^{-7}$ m s^{-1}. This gives a minimum contaimination figure of 0.1 m $(s\ torr)^{-1}$. Yb like Dy sublimes which is the reason for the poor figure. This low figure combined with Yb's high reactivity is likely the cause of the poor reproducibility. It is also quite possible that Yb reacts weakly with the substrate. This explanation is appealing as the film ratios significantly exceed that of the bulk metal reported by Curry et al. (1960). However, an interesting and unexplained effect was found on [illegible] (1960)]. However, an interesting and unex[illegible]

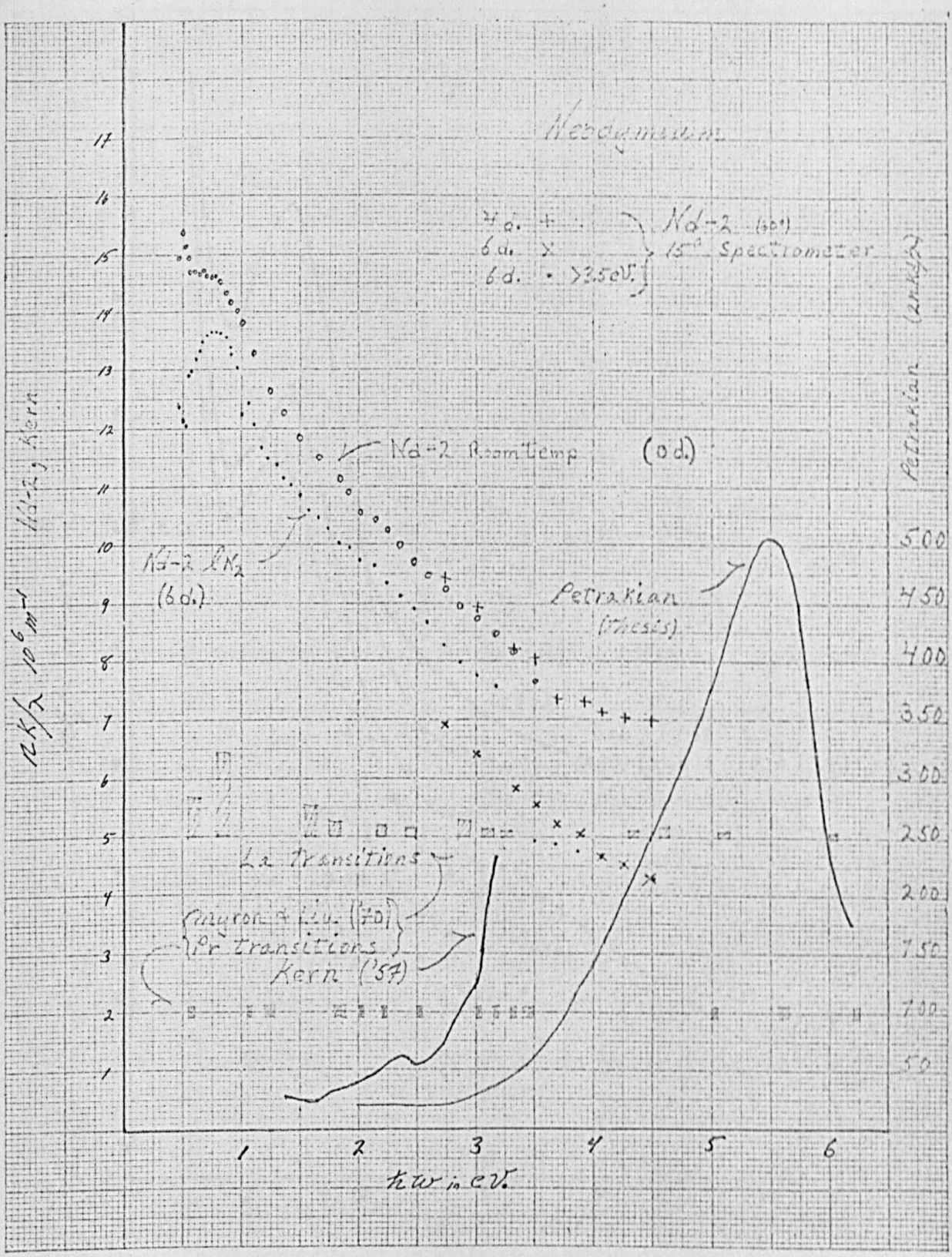

Fig. 4.7 Neodymium - Conductivity - Present and Previous Work

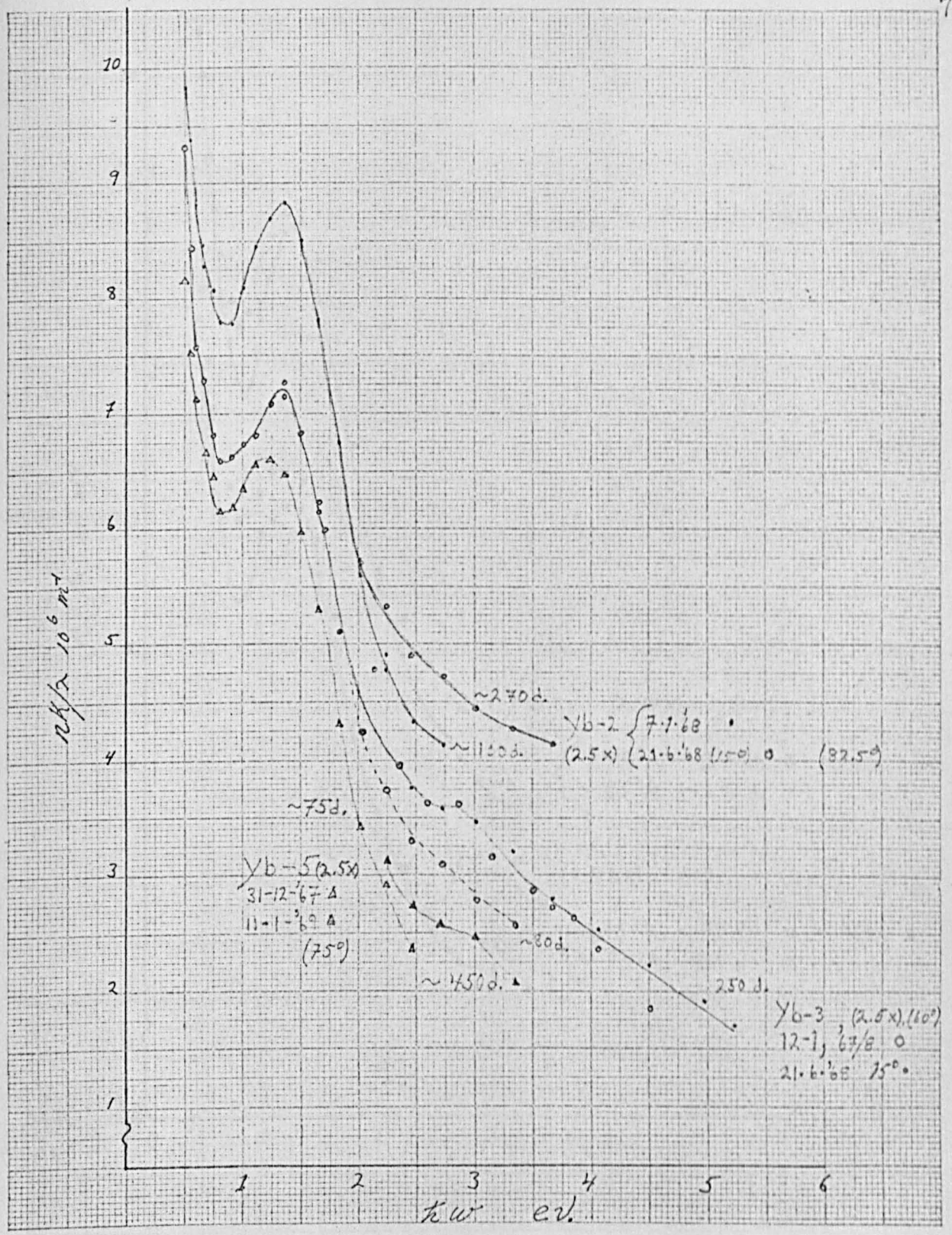

Fig. 4.8 Ytterbium - Conductivity of Three Films at 295°K

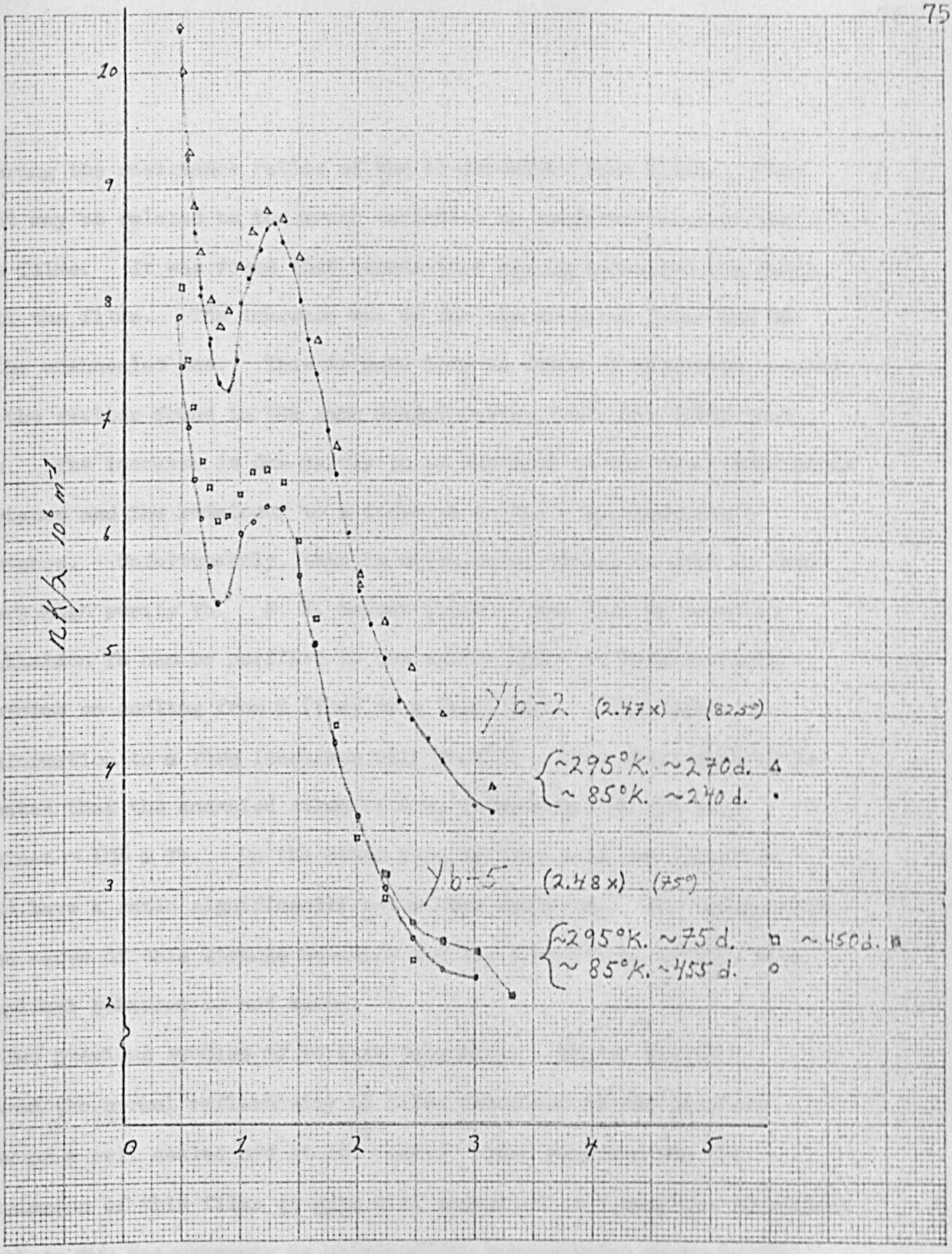

Fig. 4.9 Ytterbium - Conductivity at 85 and 295°K

measuring the resistance ratios of the co-deposited test films. This effect may be related to the great variation in conductivities of the three films. It was found that temperature cycling increased the ratio of all the films. The increase was 4% for the annealed films and 9% for the unannealed one. This is more than an order of magnitude greater than the scatter found in the same measurements of all the other test films. The increase is due partly to an increase in the room temperature resistance and the remainder to a decrease in the ℓ N_2 temperature resistance. Unfortunately, this is opposite in effect to what is found in very high purity Yb. F. X. Kayser (1970) found that by repeated distillation Yb can be purified to the extent where it spontaneously transforms on cooling from β (fcc) to α (hcp) fprm. The degree of transformation to α form increases with purity. From their data it is estimated that the annealed films at ℓ N_2 temperature should have contained $\sim$ 10% α Yb. On the other hand Yb that does not transform should have a ratio significantly below that measured. The explanation of the cause of this strange behavior and its connection, if any, with the optical behavior is not known.

Two previous studies of Yb have been made. Müller (1967) measured the normal reflectivity of films deposited on the sapphire window of a cell sealed off at 10^{-9} torr. Also measured was the transmission of thin films <u>in situ</u> also deposited on a sapphire substrate. From these two measurements he obtained the conductivity shown in Fig. 4.10. Since the conditions of deposition were not given a judgement cannot be made on whether the rather great difference with the present data is due to atmospheric contamination, reaction with the sapphire

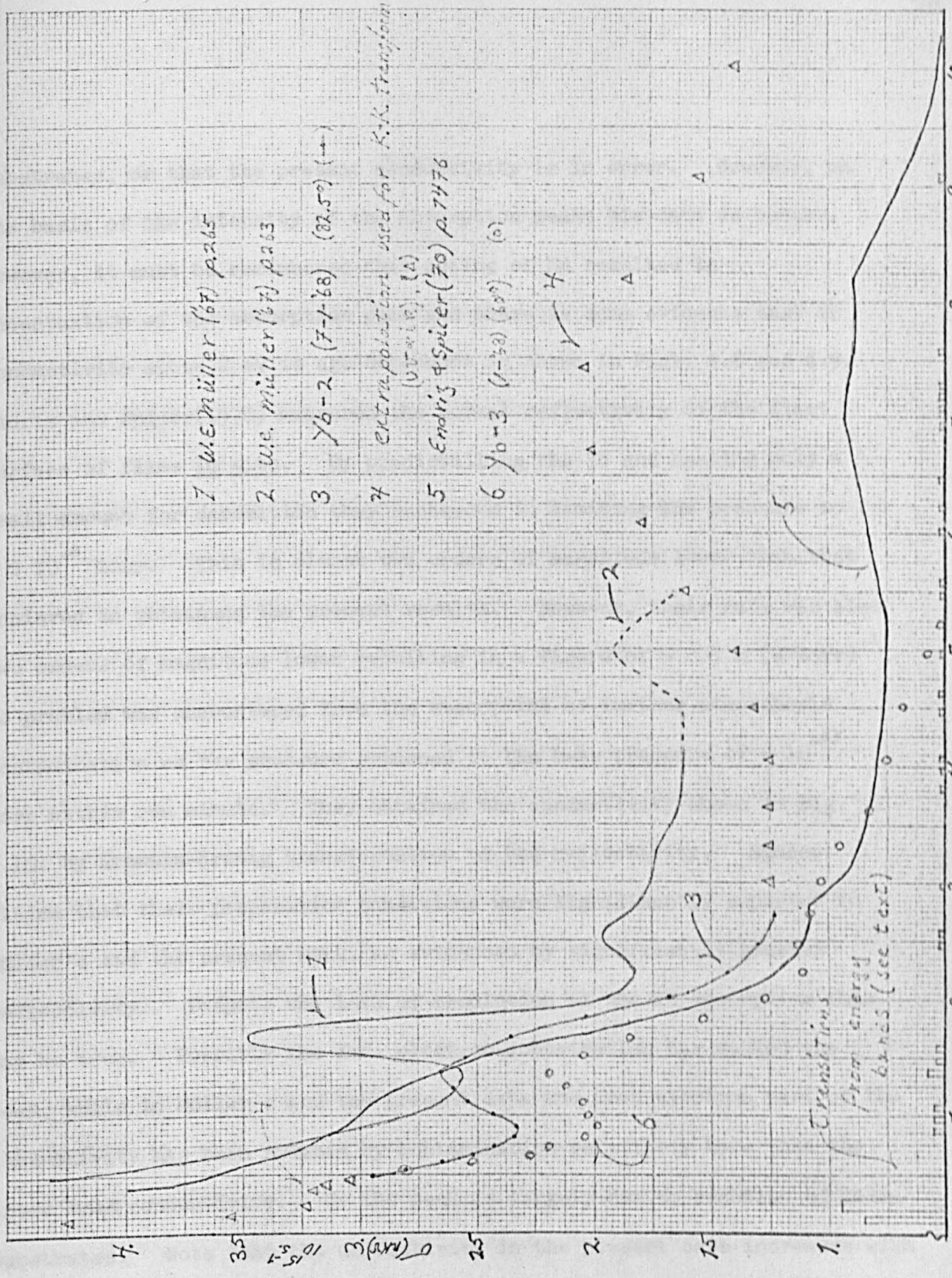

Fig. 4.10 Ytterbium - Conductivity Present and Previous Results

substrates, or that the present conductivity is in error. However, on the basis of the intensity of the absorption peaks his data is better. However, it must be remembered that ageing of Nd resulted in accentuation of the absorption peak and there is some evidence that Yb conductivity above 2 eV is age dependent as shown in Figs. 4.8 and 4.9. Endriz and Spicer(1970) measured the normal reflectivity of the first surface of films in situ. By predistilling the Yb and heating only a small amount for deposition they succeeded in limiting the pressure to $\sim 2\ 10^{-8}$ torr. This is almost two orders of magnitude lower than that achieved in obtaining the present results. However, their rate was also two orders of magnitude lower resulting in a figure of ~ 0.3 m $(s\ torr)^{-1}$. No problem was encountered from the standpoint of further atmospheric contamination as the pressure returned to the base pressure of $\sim 10^{-11}$ torr within one minute. They obtained the conductivity shown in Fig. 4.10. by Kramers-Kronig transformation of the reflectivity. Spicer claims that their preparation conditions were significantly superior to Müller's and the present work, as evidenced by significantly greater reflectivity. Despite the lack of resolution of the IR absorption this may be true. Possibly the free electron contribution has masked the peak, while in Müller's and the present data the free electron part of the conductivity has been reduced by contamination relatively more than the inter band conductivity. Or the peak is largely due to reaction with the substrates. Note that the conductivity in the present case increases with age of the film and the shortest time between preparation and measurement was 75 days. Müller's much greater conductivity might then be due to a higher reactivity of sapphire. Moreover, as discussed in Chapter 5 this conflicts with theoretically predicted conductivity.

CHAPTER 5

DISCUSSION

As would be expected from their other properties, for interpretation of their optical properties, the lanthanides fall into three groups; the heavy, and light rare earths, and the two alkaline earth metals (group II - divalent).

The HRM's are very similar to each other and in general what is found for one applies to the others. Since Gd has been examined most closely both in the past and presently, it will be used as a paradigm. It will suffice only to point out the slight variations exhibited by Dy and Tb.

On the basis of the discussion in Chapter 2 it is apparent that the conductivity of Gd is due to a free electron term and to two broad intense absorption bands. Unfortunately the "Drude" and the IR band absorptions are not well separated. This made it difficult to fit an extrapolation and leads to considerable uncertainty in its parameters. Nevertheless, the extrapolation was successful in that it allowed a K-K transform to be performed which differed with the experimental values of ϵ_1 by at most, 1.3. This occurred at the point where data was taken from different films and spectrometers and, therefore, reflects film differences. At the experimental extremes the differences were < 0.8.

An U.V. extrapolation was found necessary. This illustrates the usefulness of the K-K procedure as it predicted the uv band in reasonable agreement with that found by Petrakian, and Endriz and Spicer (a similar extrapolation was used for Yb). The parameters used to generate the IR extrapolation, and the resulting "Drude" and interband effective oscillator strengths are

tabulated in Table 5.1.

If the separation between the "Drude" and intra-band absorption is sufficiently great the optical mass may be found by plotting ϵ_1 vs ω^2. The optical mass is defined by the approximate, $(\omega/\omega_c \gg 1)$, Drude equation for ϵ_1, (eq. 5.1), $\epsilon_1 \sim \epsilon_0 - \omega_p^2/\omega_2$, where $\omega_p^2 = n_e q_e^2/k_0 m^*_{opt}$, where n_e is the elec. concentration, k_0 is the permitivity of free space, and ϵ_0 is the sum of the frequency independent sources of the dielectric constant. Unfortunately for none of the lanthanides studies was this possible.

However, for the sake of curiosity m_{opt} was found algebraically for the extrapolations. These results for Gd are included in Table 5.1. The optical mass has some significance for simple metals indicating band shape, and in comparison with the thermal mass the degree of anisotropy of the fermi surface (Abelès, 1972, Cohen, 1958). The result ($m_t/m_{opt} \sim 1.28$) indicates according to Cohen's theory a very high degree of anisotropy. The result $m_t/m_{opt} < 1$ obtains when there is extensive S_F-B.Z contact. The result is difficult to evaluate (and probably not meaningful), as the lanthanides certainly have anisotropic S_F but also have extensive B.Z. contact.

As explained in Chapter 2, two methods are available for analysing the interband absorption. The first is to fold the volume density of states about the E_F. This method has the advantage of including all transitions instead of only those at critical points. It has the concomitant diadvantage of including forbidden transitions and assumes that constant matrix elements connect the states. Fig. 4.1 shows such a folding compared with variously obtained Gd conductivities. Agreement is not very good as the second peak should have ~ 0.5 ev higher energy to agree

TABLE 5.1

Gadolinium Interband and Effective Oscillator Strength Data

σ_{DC} $19\ 10^{6}\ m^{-1}$

$\hbar\omega_c$ 0.5 ev

Photon region	f	$f_{(Drude)}$
$0 \rightarrow .45$ ev	.26	.26
$.45 \rightarrow 5.5$	1.9	.28
$5.5 \rightarrow 8.2$[1]	.93	.01
Total	3.00	.55

$m_{opt}/m_c \sim 5.4$ $\quad m_t/m_e \sim 6.9$ $\quad m_t/m_{opt} \sim 1.28$

[1] Obviously the extrapolation is too large as ω_p for the valence electron density is ~ 11.2 ev. The actual ω_p, where $f \sim 3$ is probably near 12 ev because of interband effects.

with d-band effects, (to be discussed presently). The second method is to tabulate the allowed transitions at the critical points where the joint density of states is high. Petrakian (1972) has already published a table of these permitted transitions derived from the selection rules for the group D_{6h} and band calculations supplied by J. O. Dimmock. These values have been used to make the histogram in Fig. 5.1. Except for the absence of the peak at 2 ev and that the peak near 4 ev is at too high an energy, agreement with Erskine's results is better than with the present. Erskine obtained his results by measuring the magneto-optic Kerr effect ellipsometrically. The moK effect requires that it give a different conductivity from the present results (Erskine, 1973). Erskine's explanation is now summarized. The moK effect is defined as the ellipsometric parameters (ψ and Δ) which are linear functions of the sample magnetization. This effect is dependent on spin-orbit interaction in the solid which provides a means of coupling the magnetic dipole associated with electronic spin to electric dipole transitions stimulated by incident photons. In direct analogy to the conductivity found by normal ellipsometry there are both intra and inter band components. The curve shown in Fig. 4.1 shows the experimental results with the intra-band conductivity subtracted. The difference in the "normal" and the moK derived conductivity is due to the fact that moK effect is proportional to the product of the spin-orbit interaction and the net spin polarization. Since the d and f-states probe the core-potential much more deeply than the s and p states their transitions are emphasized. In fact Erskine estimates that s-p transitions are negligible in the moK effect for Gd. On the other hand s-p transitions have large dipole matrix elements and overwhelm

Fig. 5.1 Gadolinium – Conductivity and Calculated Transitions

any structure due to d and f-states, in the normally measured conductivity. This is because the dipole matrix elements are small when $\Delta\ell$ is large. This also explains why all previous efforts to find f-states by normal optical efforts failed.

Another method of detecting f and d states is by using uv and x-ray photoemission. The use of Hi-energy photons is successful in revealing these states because these photons induce transitions to high energy states in the solid, which consequently have a higher proportion of large angular momentum. Consequently the d, and especially the f-state transitions are enhanced. Heden et al. (1971) found peaks from x-ray photoemission spectroscopy which they ascribe to initial f-states. They are shown in Fig. 5.2. As expected Eu and Gd (ℓ=0) have single peaks. Also the peaks for the LREM's show increasing binding energy with atomic number while the HREM's 4-f binding is high and approximately constant in agreement with the discussion in the introduction. Unfortunately many of the shallow peaks correspond to peaks or changes of slope in the present results. Their f-state source is confirmed by their absence in Ba and Sr (for Eu and Yb). That they are d-states if not f is evident by the fact that they are much weaker in uv photoemission. The degree of d-f nature in an initial state is shown by the magnitude of the increase in photoemission with increasing photo energy (Eastman, 1971). Heden et al. did find this true for the points found in the metals which they also measured by UPS. f → d transitions are allowed, but Fand and Cooper (Endriz, 1970), point out that transitions where $\Delta\ell$ = 1 are ~ 10 times stronger than when $\Delta\ell$ = -1.

In an effort to take this into account the band character was subjectively determined by noting the curvature about the critical point.

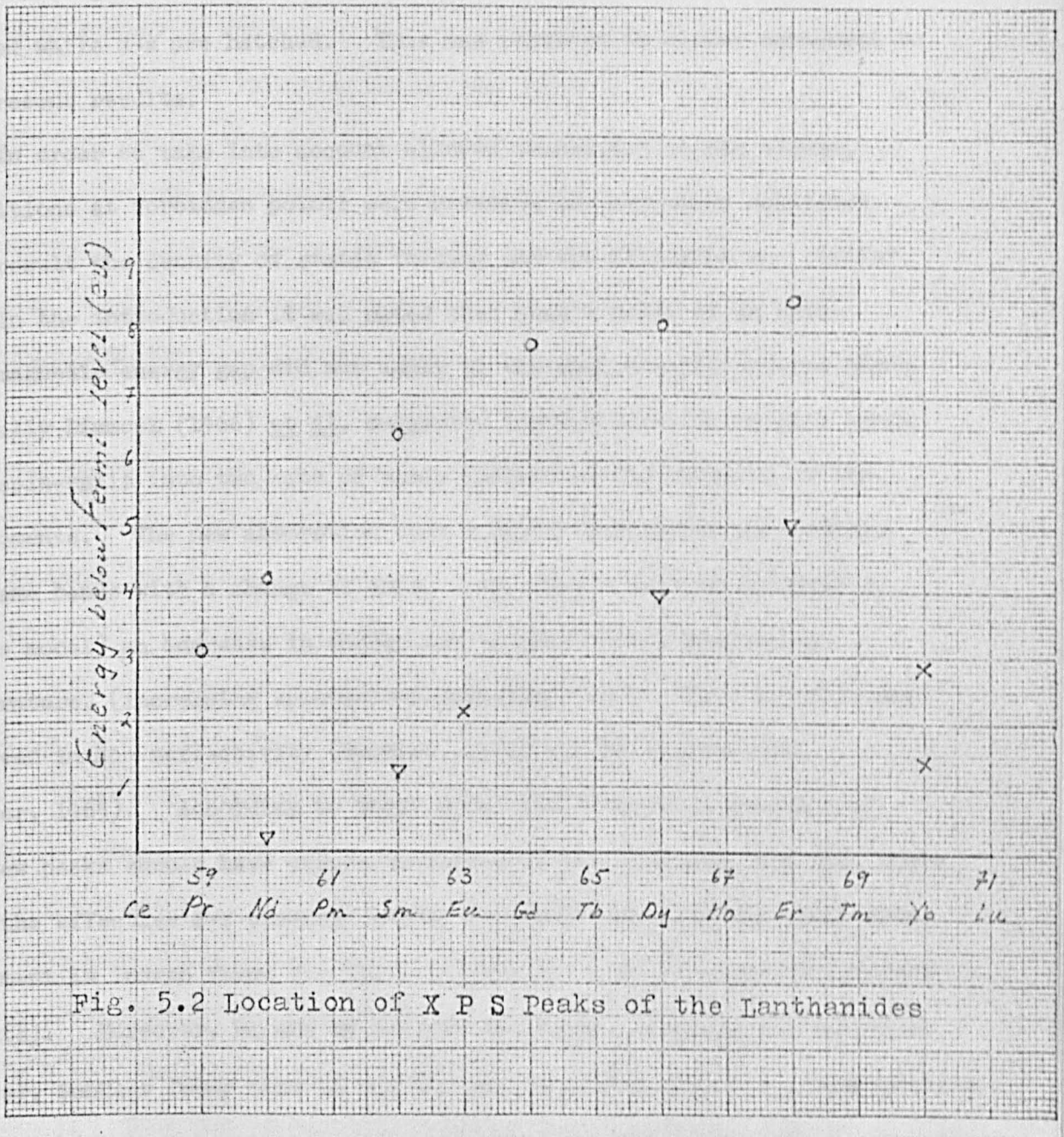

Fig. 5.2 Location of X P S Peaks of the Lanthanides

In the histogram (Fig. 5.1) transitions of s-p, p-d type are shown cross-hatched while d-s are hatched. This has resulted in closer agreement to the present results.

In order to take into account allowed transition in the volume, transitions at forbidden points were measured and are shown unhatched. As a result the density of states folding and the histogram are similar.

In the introduction it was noted that Miwa's model of an anti-ferromagnetic energy gap did not apply to the magnetically ordered REM's. Initially Dimmock (1966) et al. suggested instead that the metal's bands were spin-split into two sets of bands induced by the ordering of the 4-f moments. The new absorption then results from transitions within the same bands with a change of spin. This would lead to (similar to Miwa's model) an increase in energy and intensity with decreasing temperature, (increasing spontaneous magnetization). This behavior was observed in Hbe reflectivity (Schüler, 1964) and Dy transmission (Cooper, 1965). According to their model the saturation energies of the new peaks should have values according to the equation, $E = 2SJ$, where J is the effective s-f exchange energy ($\sim .087R$), and S is the ionic spin. Agreement is indeed found for Ho, (.35 ev), Dy, (.44 ev), and Gd (present results). Moreover, Ho and Dy exhibit the correct temperature behavior. However, Schüler found that Gd had the opposite behavior, i.e., transmission changes shift to lower energies with decreasing temperature with a saturation value of $\sim$ 0.4 ev. The initial agreement was only fortuitous since Schüler suggested and H. Liu (private communication) insists that such transitions are forbidden. Furthermore the present results show new absorption bands for Gd, Tb, and Dy at 0.67, 0.91, and 1.01 ev.* Tb and Dy's positions are

*Not necessarily to the exlusion of the previously found anomalies

$\sim$ 0.5 ev, too high for Dimmock's model. However, the present results are approximately in conformity to Dimmock's calculated bands. As it can be shown that the splitting causes the appropriate emptying and filling of bands near the E_F thereby, the IR absorption is radically changed by the creatinn of new transitions in the ferromagnetically ordered state and the removal of others that existed in the paramagnetic state. This mechanism is particularly satisfying as it explains the reduction of conductivity in the narrow region between the two peaks in the ordered state.

Spin-split bands have not been calculated, but Liu suggests (private communication) that a good approximation may be obtained from the paramagnetic bands by rigidly splitting them an amount given by the equation: $\Delta E \sim 2(g-1)J\, I_{(0)}$, (g is the Lande factor, J the ion core angular momentum, and $I_{(0)} \sim 0.074$ - assumed a constant for the HREM's). Accordingly ΔE for Gd, Tb, and Dy have the values 0.52, 0.44 and 0.37 ev. The splitting was done, simply by drawing in Figs. 5.3a,b,c new fermi levels at $E_F' = E_F \pm \Delta E/2$. Changes can be seen to occur at the critical points: K, T, Σ, U, L, S', S and P. Transitions at most of these points are forbidden, but for the same reason that forbidden transitions were included in the previous histogram all IR transitions will be considered. They are listed in Table 5.2. Two histograms made from these values are shown in Figs. 4.2 and 4.4. They were weighted by $1/\hbar\omega$. The agreement with the measured conductivity of Gd films (using all the transition changes) is indeed remarkable. However, this may only be fortuitous as explained below. Agreement with Dy* is even better when the effect of indirect transitions are taken into

*Less than half the number of transitions are changed upon ordering.

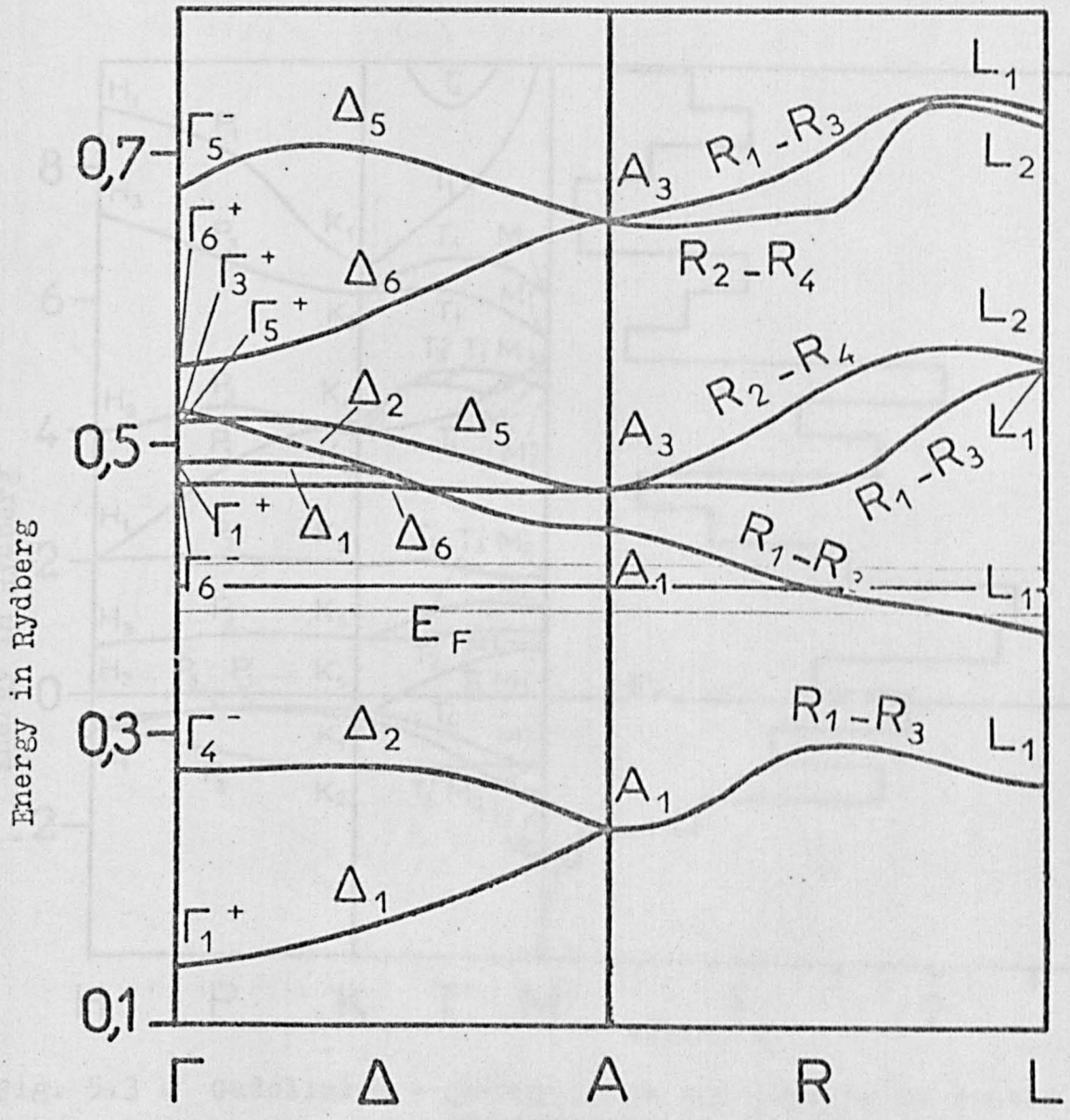

Fig. 5.3 a Gadolinium - Energy Bands According to Dimock (Petrakian - 1972 Thesis)

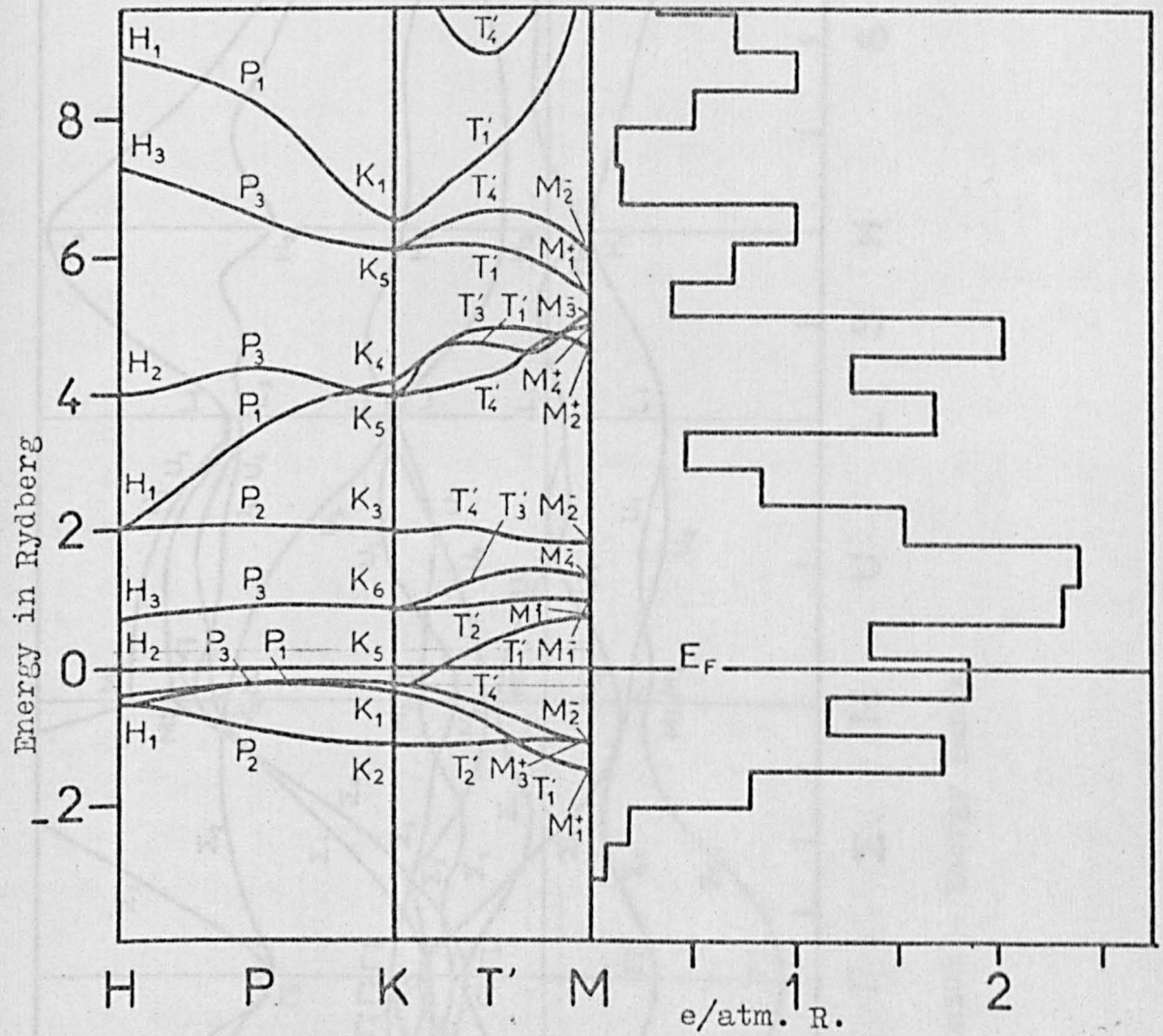

Fig. 5.3 b Gadolinium - Energy Bands and Density of States According to Dimock (Petrakian)

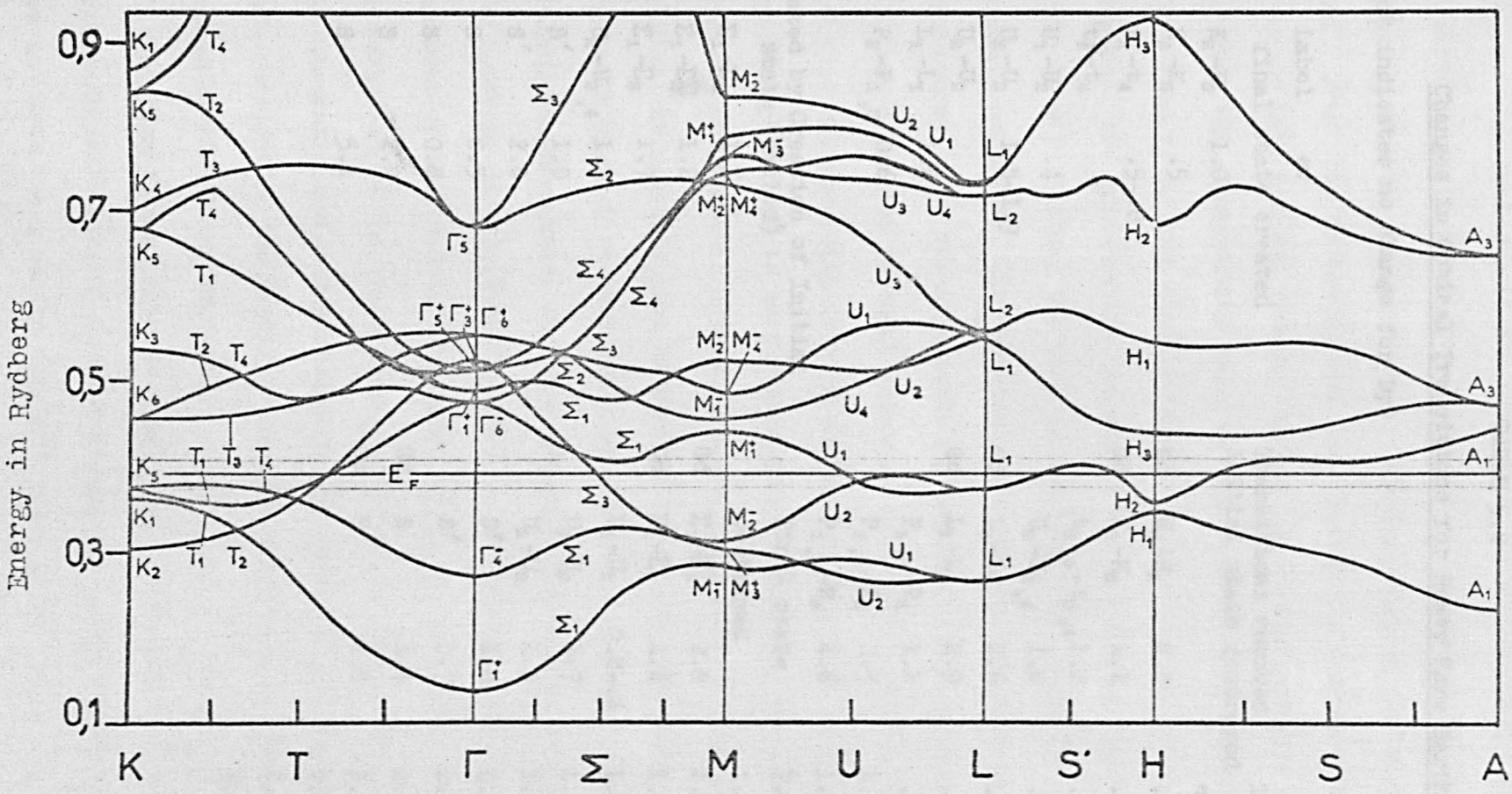

Fig. 5.3 c Gadolinium - Energy Bands

TABLE 5.2

Changes in Optical Transitions for Heavy Rare Earth Metals

("Gd" indicates no change for Dy)

	Label final state created	ev
Gd	K_2-K_5	1.0
Gd	K_1-K_5	.5
	t_2-t_4	.5-.8
	t_1-t_4	
	U_1-U_2	.4
	U_2-U_2	1.5-1.9
	U_2-U_2	
Gd	L_1-L_1	1.6
Gd	$P_2-P_{1,3}$	0.6
	Created by Creation of Initial State (filled)	
Gd	$\Sigma_1-\Sigma_1$	1.1
Gd	$\Sigma_1-\Sigma_2$	1.2
Gd	$\Sigma_1-\Sigma_3$	1.7
Gd	$U_2-U_{2,4}$	1.7
	S'	1.0
	S'	2.8
Gd	S	0.5
Gd	S	0.8
Gd	S	2.2
Gd	S	5.1

Transitions removed initial state destroyed			Tabulated total change ev	Δ	~ Δ/ω
Gd	K_5-K_3	2.2	.3	-1/2	-1.7
Gd	K_5-K_6	1.1	.4	1/2	+1.3
	$t_{1,4}-t_{3,4}$	1.2	.5	2	4
	$U_2-U_{2,4}$	1.8	.6	3	5
Gd	L_1-L_1	2.6	.7	1	1.4
Gd	L_1-L_2	2.9	.8	1	1.3
	$P_{1,3}-P_3$	1.2	.9	0	0
	$P_{1,3}-P_2$	2.3	1.0	1.5	1.5
	$P_{1,3}-P_3$	4.6	1.1	-1.5	-1.4
	final state		1.2	-5	-4.2
	destroyed		1.3	0	0
Gd	$\Sigma_1-\Sigma_1$	2.8	1.4	-1.5	-1.1
Gd	$\Sigma_1-\Sigma_1$	1.4	1.5	0	0
	U_1-U_2	0.2-.4	1.6	+2	+1.2
	U_1-U_2	1.7	1.7	+1	+6
	U_2-U_2	1.9	1.8	-2	-1.1
	S'	1.0	1.9	-1	-.5
	S'	1.7	2.0	-1/2	-.3
Gd	S	1.4	2.2	-1	-.4
Gd	S	2.0	2.4		
			2.6	-2	-.8
			2.8		
			3.0	-3	-1.0

account. An estimate of the importance of the thermally assisted transitions can be found from Nb and Yb. In general the Valley is reduced $\gtrsim$ 5% while the peak $\lesssim$ 1 to 10% depending on the quality of the film. From this it can be seen that though the conductivity does not appear to have changed from 0.5 to 0.9 ev, it has probably increased 5% over what the conductivity would be expected without magnetic order. If the film is of high quality then at 1.5 ev the reduction is $\sim$ 15%. Therefore, the ratio of the changes at 0.5 and 1.3 ev (absolute values) should be $\sim$ 3. Since the peak in the negative change (at 1.3 ev) is thermally broadened, (it represents the absence of transitions at low temperature), this value is quite reasonable. Note that Fig. 3.2 shows Dy-X (curve-labeled "without shield- $\sim 10^{-2}$ Torr ") weakly magnetized. At 0.5 ev the reduction is $\sim$ 5% while at $\sim$ 1.3 ev it is only 2%.

This agreement is very encouraging. However, the problem of the source of the magnetic effect cannot be considered solved as Dimmock's calculations probably have an uncertainty in the placement of the s-d bands with respect to each other of $\sim$ 0.02 R (.27 ev). Also the necessity of using an approximate exchange potential introduces another uncertainty of $\sim$ 0.04R (0.54 ev) (Watson, 1968). Furthermore, the decision on the placement of the bands with respect to the E_F is rather subjective as is the weighting of the transitions according to degeneracies. The assumption that thermally assisted transitions are important in this model is probably good, considering the degree of thermal broadening and the increase in conductivity with temperature.

The final question to be considered is transitions within the f-shell. Lanthanide salts exhibit intense absorption lines in the visible, but they have not been found in the metals. Kern (1957) calculated that his

apparatus should detect such transitions if their oscillator strengths are as great as in the salts. He verified that his spectrometer and detector etc. were sufficiently sensitive by recording the spectra of several salts with his apparatus. Evidently the f-f transitions are weaker or masked by the other metallic absorption. The sensitivity of his apparatus for nk was about the same as the one used in the present work ($\Delta nk \sim 0.1$), but the resolution was almost an order of magnitude better than used in the present measurements in the visible. Therefore, it is not surprising that no evidence of f-f transitions were found.

Neodymium

Unfortunately, no energy band plots or density of states histograms have been published for Nd; however, Myron and Liu (1970) have published both energy bands and density of states histograms for f.c.c. La and Pr. Since Nd is a hcp metal at the measurement temperatures agreement is not expected to be good, however, transitions were determined as well as a density of states folding for both. In Fig. 5.4 JODS histograms for La and Pr are shown, while in Fig. 4.7 optical data is compared to direct transitions. In both cases there is considerably better agreement with the conductivity derived from calculations for La than for Pr. If the low lying XPS peak (Fig. 5.2) in Nd is due to a d-band instead of an f-state then Nd might be expected to be more similar to La than Pr. This is because the f-state is more loosely bound in Pr than in Nd. As a result Pr's bands near the E_F are distorted by the f-electrons more than are La's. This assumes that the unoccupied state is sufficiently remote. This agreement is supported by the fact that Nd's conductivity peak is in between Pr's and the HREM's, whose f-states interact minimally with the

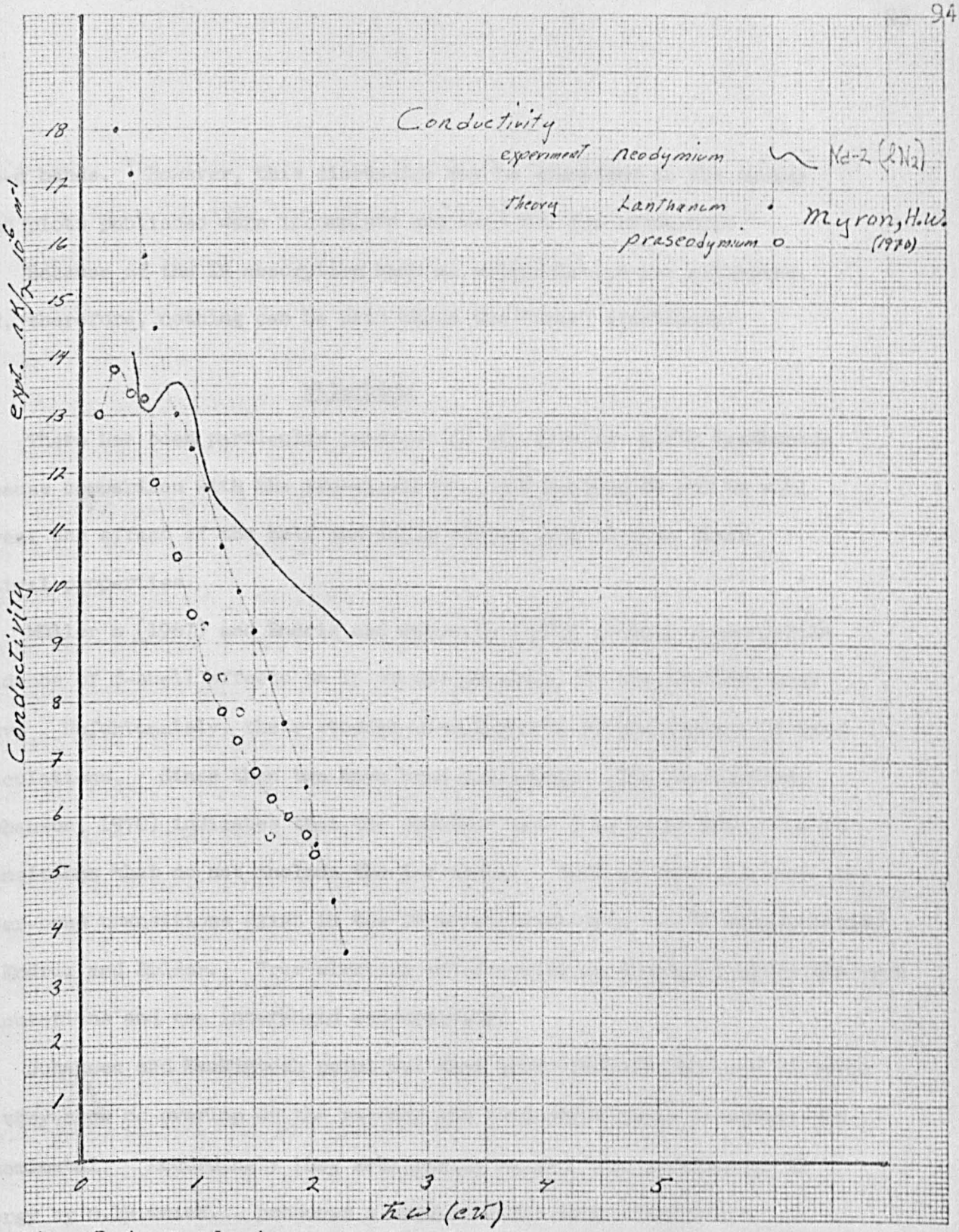

Fig. 5.4 Neodymium - Conductivity and Joint Density of States of Lanthanum and Praseodymium Comparred

s-p-d bands. However, this discussion may be premature as the energy band plots published were incomplete and were for fcc structure.

Because of the IR absorption band no extrapolation was attempted, and, therefore, nothing can be said about the "free" electrons.

Ytterbium

There has been particular interest in the alkaline earth lanthanide because comparison with the iso-electronic, and-morphic Ba and Sr will reveal the effect of the half and fully filled f-shell upon their optical properties.

Müller's (1967) and Endriz and Spicer's (1970) studies found little evidence of f-shell effects on Yb except possibly for the shoulder near 3 ev. Unfortunately, their studies were hampered by the absence of band calculations. Since then two have been published. The earlier one, (Johanson, 1970) indicates that the shoulder near 3 ev is probably due to transitions that do not include the 4-f shell. Both of them indicate that inter-band transitions exist in the IR which invalidate the IR extrapolation of Endriz and Spicer. Free-electron effects will be discussed after the band calculations and the interband conductivity.

Johansen and Mackintosh point out that their calculations are in error as they show no overlap of the valence and conduction bands necessary for a semimetal. Accordingly they arbitrarily raised "the d-resonance in energy by 0.1R which... produces a semi-metallic band structure." Unfortunately, only two of the bands are shown with this change. Also the E_F is not given. However, this change will not eliminate the transitions below 0.5 ev and probably serves to lower the energy of the groups of transitions at 1 and 1.5 ev while leaving the transitions above 3 ev relatively

unchanged. The transitions taken from their unmodified energy bands are shown in Fig. 4.10, (the transitions below 3.0 ev have been energy weighted). As with the HREM's there are transitions in the 3-4 ev region which do not correspond to optical conductivity. Again the explanation given for the HREM's may apply.

Jepson and Anderson's (1971) results are considerably better in that the bands overlap at the E_F, and, furthermore, their calculated extremal areas of the S_F agree well with measured dH vH frequencies. However, they found that better agreement would be obtained if the d-band was lowered by $\sim$ 0.14 ev. This will reduce the energy of the 1R transitions (shown in Fig. 5.5) by nearly the same amount resulting in excellent agreement with the presently obtained conductivity. Again it must be stressed that all the transitions were given equal weight regardless of selection rules. Also the 1970 calculated bands were for fcc Yb and the 1971 for HCP. What structure the films had is not certain, but evidently any error in comparing the films to the wrong structure is negligible compared to errors in the band calculations. Since the bands at only about half of the critical points were given, it is possible that the agreement is illusory.

Attempts to fit a "Drude" extrapolation directly to the experimental conductivity failed. It was thought that this was due to two band conduction with different masses, and scatter times. Accordingly a two band Drude extrapolation with D.C. conductivities of 90 10^6 m^{-1} and 10 10^6 m^{-1} and with inverse scatter times, respectively, of 0.04 and 0.7 ev gave satisfactory K-K agreement. However, this is quite unreasonable as it implies an order of magnitude difference in effective mass and scatter

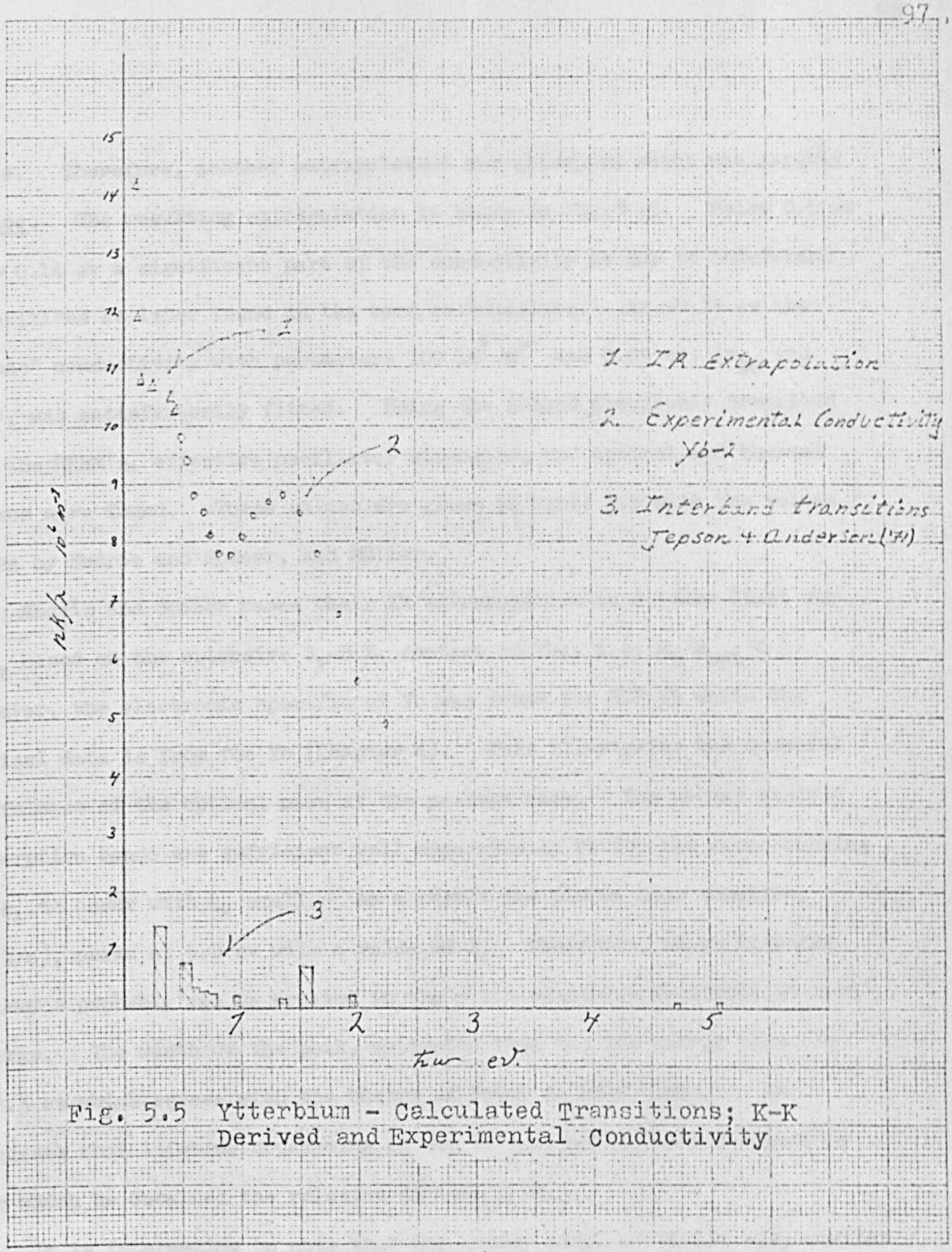

Fig. 5.5 Ytterbium - Calculated Transitions; K-K Derived and Experimental Conductivity

times. Therefore, another extrapolation was attempted which was largely ad hoc. The resulting extrapolation is shown in Fig. 5.5. Below 0.5 ev to ~ 0.14 ev a significant part of the conductivity is due to inter-band transitions as later found in the band calculations. At ~0.14 ev the "Drude" conductivity with parameters 100 10^6 m^{-1} and 0.05 ev, (σ_{DC} and $\hbar\omega_\theta$), was satisfactorily fitted. Using the method previously described for the HREM's, effective oscillator strengths, and optical and thermal masses were found. These values are given in Table 5.3 with the values given by Endriz and Spicer, and Müller.

Endriz and Spicer based their IR extrapolation on a lower limit for m_{opt} based on the extensive S_F-B.Z. contact in Yb., i.e. $m_t/m_{opt} < 1$. However, the electronic specific of Yb was found for HCP Yb while the optical data is from fcc Yb (Chapter 4). This illustrates the doubtful usefulness of the optical mass at the present time. The uv and visible absorption bands are sufficient well separated in Yb for the zero crossing of ϵ_1 to occur with ϵ_2 small. As a result the plasma loss function, $Im(1/\epsilon)$, peaks at 5.0 ev with a value of 1. Therefore, short lifetime plasmons probably can be created in the ~ 1.4 electrons available at that energy. The width of the peak, estimated from the low energy side, is ~ 2.3 ev which agrees with the theory of Peter A. Wolf (1953). He suggests that lifetime broadening is due to interaction with d-electrons for which he obtained the relation $\Delta E \sim \hbar\omega_p\epsilon_2/2$.

It is interesting to note that the energy bands of Yb are very similar to those of the HREM's with the E_F falling in a pronounced dip in the density of states. This is shown in Fig. 5.6 which indicates that there should be conductivity peaks at ~ 1.2, and 2.5 ev. Except that the 2.5 ev peak is very weak, (possibly for the reason discussed earlier for Gd), this is indeed the behavior of Yb.

TABLE 5.3

Ytterbium

Data from Drude extrapolation:

	Present results	Endriz and Spicer	Müller
σ_{DC}	$100\ 10^{6}\ m^{-1}$ ($310^{16} s^{-1}$)	$3.16\ 10^{16} s^{-1}$	-
$\hbar\omega_c$	0.05 ev ($7.6\ 10^{13} s^{-1}$, 1.310^{-14} s)	(0.127 ev) $5.18\ 10^{-15}$ s	-
f_{Drude}	0.37 e/atm	~ .1 e/atm (.94 c/atm)[1]	0.4 e/atm
$\hbar\omega_p$(Drude)	3.52 ev	-	-

m_t/m_e = 2.26(HCP) / 5.73(fcc) m_{opt}/m_e = 5.4 m_t/m_{opt} $.42_{HCP}/1.06_{fcc}$

f		
	.45 e/atm	0-0.5 ev
	.96	0.5-5.5 ev
	~ .6	UV ~ 8 ev[2]

[1] From the sum rule using σ_{DC} and τ.

[2] As with Gd this value is too small as the free electron plasma frequency for Yb is 8.16 ev. This agrees with Endriz and Spicer's conductivity above 4 ev. An extrapolation fitted to By-3 instead of Yb-2 would probably give a satisfactory result (see Fig. 4.10)

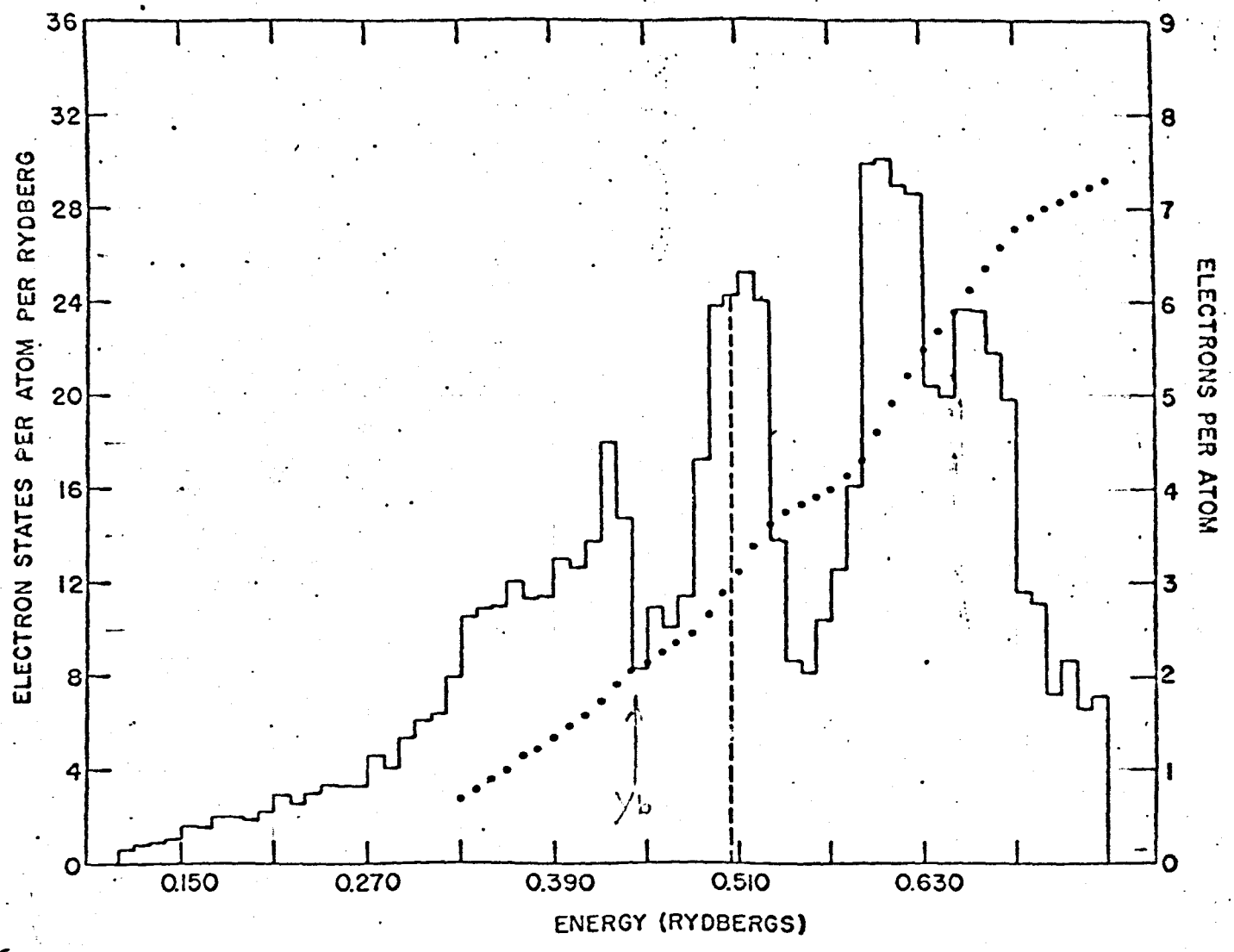

Fig. 5.6 Dysprosium density of states histogram. The dotted curve is the intergrated density of states curve with the units on the right hand side. (supplied by S. H. Liu)

It is felt that this work has made a distinct advancement in the understanding of the electronic structure of the magnetic REM's. This is because previously no satisfactory explanation existed for the optical conductivity changes due to magnetic order. Though the necessary theoretical information for this explanation has been available for some time, it was never suggested probably because the necessary optical measurements were insufficiently extensive and accurate. Unfortunately insufficient time was available to confirm this model by measuring other of the metals which would be ordered at liquid nitrogen temperature. Particularly appropriate would be europium and holmium. Eu has the same spin energy splitting as Gb, but is divalent and, therefore, probably has nearly the same structure as Yb. Therefore, ordered Eu and cooled Yb may be directly compared as Yb would represent Eu without magnetic order. Comparing the expected effect of the splitting with measured conductivity would be an especially critical test of the explanation. This is because the unsplit Fermi level is approximately 0.95eV lower than in the HREM's, (see Fig. 5.6). Assuming a rigid band model Figs. 5.3 might be used. Of course the position of the critical points would be inaccurate as Eu is BCC while the HREM's are HCP. Alternatively both published bands for Yb could be tried.

Holmium with a splitting of ~0.3eV would be expected to behave similarly to Dy but with less change upon ordering.

Little can be said about neodymium until band structure calculations are available. Nd may prove to be a critical test of these calculations because of the rich structure in the near I.R.

Also the validity of the ytterbium measurements could not be determined because of the lack of agreement with Müller's and Endriz's results. However, agreement with calculated bands is good and the position of the structure agrees with Endriz's. Remeasurement needs to be done to determine the effect of ageing.

REFERENCES

Abeles, F. (ed.) (1966), "Optical Properties and Electronic Structure of Metals and Alloys", North Holland Publishing Co., Amsterdam.

Abeles, F. (ed.) (1972), "Optical Properties of Solids", North Holland Publishing Co., Amsterdam.

Anderson, G. S., Sam Legvohd and F. H. Spedding, (1958), Phys. Rev., 111, 1257.

Bennett, H. E. and Jean M. Bennett, "Physics of Thin Films", 4, Academic Press, New York (1967).

Bucher, E. (1969), Phys. Rev. Letters, 22, 1260.

Bucher, E. (1970), Phys. Rev, B., 2, 3911.

Cohen, M. M. (1958), Phil. Mag., 3, 762.

Colvin, R. V. (1960), Phys. Rev., 120, 741.

Conn, G. K. T. and G. K. Eaton (1954), J. Opt. Soc. Amer., 44, 546.

Cooper, B. R. and R. W. Redington (1965), Phys. Rev. Letters, 14, 1066.

Curry, M. A., S. Legvold, F. H. Spedding (1960), Phys. Rev., 117, 953.

Dimmock, J. O. and A. J. Freeman (1964), Phys. Rev. Letters, 13, 750.

Dimmock, J. O. (1966), see Abeles, F. (1966).

Dimmock, J. O. (1971), "Solid State Physics", Volume 26, Academic Press, New York.

Eastman, D. E. (1971), Journal of Applied Physics, 42, 1396.

Ehrenreich, H. and H. R. Philipp (1962), Phys. Rev., 128, 1622.

Ehrenreich, Philipp and D. J. Olechna (1963), Phys. Rev., 131, 2469.

Elliott, R. J. (1954), Phys. Rev., 94, 564.

Endriz, J. G. and W. E. Spicer (1970), Phys. Rev. B., 2, 1466.

Erskine, J. (1972-1973), Private Communication and preprint Phys. Rev., 1973.

Fenstermaker, Carl A. and Frank L. McCrackin (1969), Surface Science, 16, 85.

De Gennes, P.G., (1962), Le Journal de Physique et le Radium, 23, 510.

Green, R.W. (1961), Phys. Rev., 122, 827.

Gustafson, D. R. and A. R. Mackintosh (1964), J. Phys. Chem. Solids, 25, 389.

Harbeke, Günther (1972), see Abeles, F., 1972.

Heden, P. D. (1971), Phys. Rev. Letters, 26, 432.

Hodgson, J. N. (1962), J. Phys. Chem. Solids, 23, 1737.

Hodgson, J. N. (1967), "The Solid-Gas Interface", E. Alison Flood (ed.), Marcel Dekker Inc., New York.

Hodgson, J. N. (1970), "Optical Absorption and Dispersion in Solids", Chapman and Hall Ltd., London.

Ives, Herbert E. and H. B. Briggs (1936), Journal of the Optical Society of America, 26, 238.

James, N. R. et al. (1952), Phys. Rev., 88, 1092.

Jepson, O., and O. K. Anderson (1971), Solid State Comm., 9, 1763.

Johanson, G. and A. R. Mackintosh (1970), Solid State Comm., 8, 121.

Kasuya, Tadao (1956), Progress of Theoretical Physics (Japan), 16, 58.

Keyser, F. X. (1970), Phys. Rev. Letters, 25, 662.

Kern, Eberhard (1957), Zeitschrift für Physik, 148, 38.

Kevane, C. J., S. Legvold and F. H. Spedding (1953), Phys. Rev., 91, 1372.

Knyazev, Yu. V. (1970), Phys. M. and Metall., 30, 230.

Knyazev, Yu. V. (1971), Fiz. Met. Metalloved., 31, 1099.

Knyazev, Yu. V. (1971a), Fizica Met. Metalloved., 32, 1189.

Koehler, W. C. (1965), Phys. Rev., 126, 720.

Koehler, W. C. (1965a), J. Appl. Phys., 36, 1078.

Kruger, Jerome and H. T. Yaken (1964), Corrosion, 20(1) 29t.

Landau, L. N. and E. M. Lifshitz (1963), "Electrodynamics of Continuous Media", Pergamon Press, Oxford.

Liljenvall, H. G. et al. (1970), The Philosophical Mag., 22, 243.

Mackintosh, A. R. (1962), Phys. Rev. Letters, 9, 90.

Malitson, I. H. (1965), Journal Opt. Soc. Amer., 55, 1205.

Miwa, Hirosi (1961), Progress of Theoretical Physics (Japan), 26, 693.

Miwa, Hirosi (1963), Progress of Theoretical Physics (Japan), 29, 477.

Moss, T. S. (1959), "Optical Properties of Semi-Conductors", Butterworths Scientific Publications, London.

Müller, W. E. (1967), Phys. kondens. Materie, 6, 243.

Myron, H. W. and S. H. Liu (1970), Phys. Rev. B., 1, 2414.

Pells, G. P. and M. Shiga (1969), Journal of Physics C., 2, 1835.

Petrakian, J. P. (1972), Journal Opt. Soc. Amer., 62, 401 and Ph.D. Thesis.

Price, D. J. (1946), Proc. Phys. Soc. (London), 58, 704.

Rodda, J. L. and M. G. Stewart (1963), Phys. Rev., 131, 255.

Schüler, C. C. (1964), Physics Letters, 12, 84.

Schüler, C. C. (1966), see Abeles, F., 1966.

Shiga, M. and G. P. Pells (1969), J. Phys. C. (S. S. Phys.) 2.

Stern, Frank (1963), Solid State Physics, 15, 299, Academic Press, New York, London.

Tannhäuser, Armin (1962), Z. Physik., 170, 533.

Watson, R. E. (1968), Phys. Rev., 167, 497.

Williams, R. W. and A. R. Mackintosh (1968), Phys. Rev., 168, 679.

Wolf, Peter A. (1953), Phys. Rev., 92, 18.

Wybourne, Brian G. (1965), "Spectroscopic Properties of Rare Earths", Interscience Publications, New York.